NUMERICAL STUDY ON THE BEHAVIOUR OF CFRP AND BFRP STRENGTHENED RC BEAM-COLUMN JOINT WITH BEAM OPENING UNDER CYCLIC LOADING

THESIS REPORT

Submitted by

ASHOK S

TKM21CESC06

to

the A P J Abdul Kalam Technological University

in partial fulfilment of the requirements for the award of the Degree

of

Master of Technology

in

Structural Engineering & Construction Management

DEPARTMENT OF CIVIL ENGINEERING

TKM College of Engineering, Kollam

JULY 2023

DECLARATION

I undersigned hereby declare that the project report, "**NUMERICAL STUDY ON THE BEHAVIOUR OF CFRP AND BFRP STRENGTHENED RC BEAM-COLUMN JOINT WITH BEAM OPENING UNDER CYCLIC LOADING**", submitted for partial fulfilment of the requirements for the award of the degree of Master of Technology of the APJ Abdul Kalam Technological University, Kerala is a bonafide work done by me under supervision of **Dr. Rekha Ambi,** Assistant Professor, Department of Civil Engineering. This submission represents my ideas in my own words and where ideas or words of others have been included; I have adequately and accurately cited and referenced the original sources. I also declare that I have adhered to ethics of academic honesty and integrity and have not misrepresented or fabricated any data or idea or fact or source in my submission. I understand that any violation of the above will be a cause for disciplinary action by the institute and/or the University and can also evoke penal action from the sources which have thus not been properly cited or from whom proper permission has not been obtained. This report has not been previously formed the basis for the award of any degree, diploma or similar title of any other University.

Place: Kollam Ashok S

Date: 12-07-2023

DEPARTMENT OF CIVIL ENGINEERING

T.K.M. COLLEGE OF ENGINEERING, KOLLAM

CERTIFICATE

Certified that this report entitled **'NUMERICAL STUDY ON THE BEHAVIOUR OF CFRP AND BFRP STRENGTHENED RC BEAM-COLUMN JOINT WITH BEAM OPENING UNDER CYCLIC LOADING'** is the report of thesis presented by ASHOK S.**, TKM21CESC06** during **2022-2023** in partial fulfilment of the requirements for the award of the Degree of Master of Technology in Structural Engineering & Construction Management of the A P J Abdul Kalam Technological University.

Guide	Project coordinator	Head of the Department
Dr. Rekha Ambi Assistant Professor Dept. of Civil Engg.	**Dr. Kavitha Madhu** Associate Professor Dept. of Civil Engg.	**Dr. Sajeeb R** Professor Dept. of Civil Engg.

ACKNOWLEDGEMENT

I take this opportunity to express my deep sense of gratitude and sincere thanks to all who helped me to complete the project successfully.

I am deeply indebted to my guide, **Dr. Rekha Ambi,** Assistant Professor, Department of Civil Engineering for her excellent guidance, positive criticism and valuable comments.

I am thankful to my Project coordinator, **Dr. Kavitha Madhu,** Associate Professor, Department of Civil Engineering for her constant supervision as well as for providing necessary information regarding the project.

I am greatly thankful to **Dr. Sajeeb R**, Professor and Head of the Department of Civil Engineering, for his kind support.

Finally, I thank my family and friends who directly and indirectly contributed to the successful completion of my project.

ASHOK S

ABSTRACT

Beam-column joint is the most important part of any framed building structure. In many cases due to mechanical, electrical and plumbing needs openings are made in beam column joint at transverse beam section. Many times, these openings are made without checking the strength requirement of joint. Presence of these opening may cause detrimental effect on structure especially considering the effect of seismic loads. Which brings in the requirement of strengthening of the beam-column joint to prevent premature failure resulting in endangering the life of people and structure. The various strengthening techniques used of discussion are; fibre reinforced polymer (FRP) composites, Ferrocement, Steel plate etc. The purpose of this study the efficiency of retrofitting beam-column junctions with transverse beam opening a with Carbon Fiber Reinforced Polymer (CFRP) and Basalt Fiber Reinforced Polymer (BFRP). Analysis can be done numerically to assess the performance of the original and improved joint models using nonlinear finite element analysis. The performance has been investigated in terms of load carrying capacity, deflection, failure pattern and displacement ductility. The parameters of study include; Size, shape, distance of opening from joint and thickness of FRP used.

Keywords: Beam Column Joint, Strengthening, CFRP, BFRP, Openning.

CONTENTS

LIST OF FIGURES

LIST OF TABLES

Chapter 1
Introduction

1.1 General

Reinforced cement concrete (RCC) infrastructures are among the most common building structures. Most of the damages to existing reinforced concrete infrastructure are due to inadequate design, poor maintenance, overloading, earthquakes, explosions, and fire. All these factors lead to strength deficient structures, which results in large deformation. Hence strengthening/retrofitting of such structures has become one of the most demanding construction activities. As far as RCC framed structures are concerned, the beam-column joints are crucial elements which are prone to failure. Beam column joints (BCJ) are structurally notable because they transfer both lateral forces as well as moments. Openings of different sizes and shapes are needed in reinforced concrete (RC) structures, which allow the execution of the electromechanical plumbing system, sanitation, heating, ventilation, air-conditioning, telephone and computer networks and other mechanical equipment. Figure 1.1 shows transvers beam opening in beam column joint. Allowing these ducts to pass through a transverse opening in the floor beam, instead of placing them underneath the soffit of the beam, as per electromechanical plumbing design, irrelevant of the structural aspect. Which could lead to situation where opening are nearby beam-column joints at the plastic hinge zone, resulting in high shear stresses and deformation causing premature failure beam-column joint. Because shear failure is brittle, it is not an acceptable structural performance, especially in seismic conditions. Most designer engineers permit the embedment of small pipes, provided some additional reinforcement is used around the periphery of the opening. However, when large openings are encountered, particularly in reinforced or pre-stressed concrete members, they show a general reluctance to deal with them because adequate technical information is not readily available. Since relevant specific guidelines are not provided in building codes, designs are frequently based on intuition. This may lead to disastrous consequences or unjustified additional costs especially under loads like earthquake loads.

Previous research done shows that providing reinforcement around opening, increased the failure load and reduced deformation. In case of existing beam column joint with transverse beam opening, the preferable method of upgrading is by using retrofitting

techniques. Various retrofitting techniques are available for concrete structures are concrete jacketing, steel jacketing, wrapping with fibre reinforced polymer (FRP) sheets, external prestressing etc.

Figure 1.1 Transvers beam opening in beam column joint

(Source: Amin et al 2017)

Among these strategies, fiber-reinforced polymer (FRP) composites as retrofit materials have seen significant success in recent years. The superior properties of (FRP) polymer composite materials like high corrosion resistance, high strength, high stiffness, excellent fatigue performance and good resistance to chemical attack etc., has motivated the researchers and engineers to use the polymer composites in the field of rehabilitation of structures. Retrofitting and strengthening are the most environmentally friendly and efficient ways to improve the performance of a beam column joint.

1.2 Beam Column Joint

In the case of framed structures, Beam column joint is an important element in its body structure. The area of the column that frames the column and is within the deepest

beam's depth is referred to as the beam column joint. The joints must be sturdy and rigid enough to bear the forces generated internally by the framework components. Allowing adjoining members to reach and maintain their maximum capacity is a functional requirement of a joint, which is the zone where beams and columns cross. The beam column joint is designed as per the “strong column - weak beam” philosophy, which is recommended to ensure the generation of beam plastic hinging at large displacements, rather than column hinging. The major function of the beam column junction in a reinforced concrete structure is to effectively transfer the load from connecting components under seismic and gravity loads. Particularly when the structure is vulnerable to seismic loading, it should be well designed and detailed. Brittle bond and shear failure mechanisms control the failure of reinforced concrete beam column joints during earthquakes.

Beam column joints are classified according to geometry as three types of joints as interior joint, exterior joint and corner joint as shown in fig 1.2. An interior junction is created when four beams frame the vertical faces of a column. When two other beams frame the connection from perpendicular angles and one beam frames into the vertical face of the column, the junction is referred to as an external joint. The joint is known as a corner joint when a beam frames into two neighbouring vertical faces of a column. Beams are anticipated to acquire plastic hinges at their ends and generate flexural overstrength beyond the design strength. Joints should follow a strong column-weak beam design

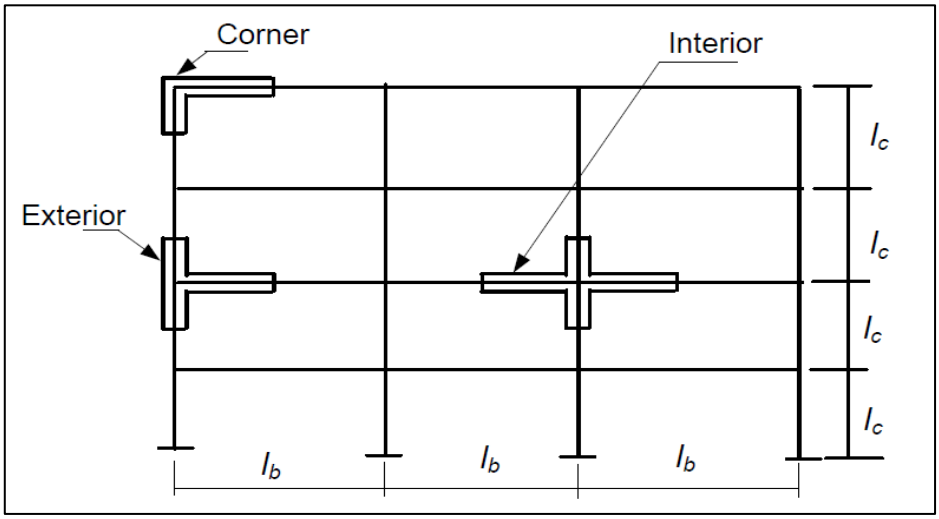

Figure 1.2 Typical frame with beam column joint

(Source: Uma and Prasad, 2015)

1.3. Carbon Fiber Reinforced Polymer

Carbon fiber reinforced polymer (CFRP) is a type of composite materials consist of carbon fiber and polymer. The carbon fiber provides the strength and stiffness while the polymer acts as cohesive matrix to protect and held the fibers together. CFRP are manufactured as a strips, bars, and sheets using different production technique. CFRP has excellent physical and mechanical properties. The tensile strength is many times stronger than that of the ordinary steel, and the modulus of elasticity is never worse than that of steel. In CFRP, the reinforcement is made of carbon fibre, which offers strength and rigidity, and epoxy, a popular polymer glue, which bonds the reinforcement in an organised manner. CFRP materials possess good rigidity, high strength, low density, corrosion resistance, vibration resistance, high ultimate strain, high fatigue resistance, and low thermal conductivity. Carbon Fiber Reinforced Polymers are most typically employed in industrial masonry structures for retrofitting of existing structures that have been damaged owing to earthquakes, chemical reactions, environmental effects, and so on. Figure 1.4 shows the CFRP fabric used for retrofitting. The effect of FRP wrapping improves the retrofitted specimens' energy absorption capacity, ductility, and stiffness. Carbon fiber Reinforced Polymers (CFRPs) are much more substantial and sustainable materials. They can be employed in strengthening damaged structural components of buildings like beams, columns etc.

Figure 1.3 CFRP fabric (Source: Sabara. et. al., 2018)

1.4. Basalt Fiber Reinforced Polymer

Basalt fibre is a bio-derived mineral fiber from volcanic rocks and has several advantages, such as good chemical resistance and mechanical properties Basalt fiber has similar tensile properties as glass fibers and has a higher maximum service temperature than glass and carbon fibers. This enables basalt fiber composites to be a viable and sustainable alternative to glass fiber composites for structural applications. Basalt fiber has good mechanical properties in combination with high temperature and alkaline resistance, basalt fiber is a good candidate for composites with thermoset matrices such as epoxy and polyester. The modulus of elasticity of basalt fabric is in the range of 85–91 GPa, which is lower than CFRP. The BFRP has a lower cost and is one of the best choices to replace GFRP and CFRP. Basalt fiber-reinforced polymers (BFRPs) have been widely used in the petrochemical, construction, aerospace, automobile, ship, and other industries. Figure 1.4 shows BFRP wrapping in beam column joint.

Figure 1.4 BFRP wrapping (Source: Sakthimurugan et al., 2021)

Chapter 2

Literature Review

2.1 General

2.1.1 Beam column joint

Among different elements, the beam-column joints have been highly susceptible to seismic excitations and the failure of joint panel has been frequently observed**.** There is a need for providing external strengthening to enhance the performance of beam column joint **(Rajaram, P. et.al., 2010)**. Studies done to investigate the crack pattern, failure mode, stiffness degradation and energy dissipation of BCJ with different size, location and aspect ratio of opening. Results showed that closer proximity of opening increased energy dissipation while increase aspect ratio reduced energy dissipation **(Amin et al 2017)**. The failure load of beam-column joints (BCJ) is significantly reduced with wider the opening closer to the column. The BCJ with reinforced opening showed increase in failure load **(Amin et al 2021).**

2.1.2 Strengthening of Beam column joints using FRP

Several studies were done to improve the performance of beam column joint by using various retrofitting techniques by using steel plates, FRP and BFRP composites. Use of steel plate prestressed by cross ties showed more ductile response and higher hysteresis energy capacity, as well as moderate strength improvement **(Adibi et al. 2017**). **Laseima et al. (2021)** has conducted an experimental study on beam column joints without joint transverse reinforcement. The external beam-column joints of the experimental specimens were strengthened with basalt fiber reinforced polymer (BFRP) and carbon fiber reinforced polymer (CFRP), respectively, to improve their seismic performance. The beam and column's cross-sections were altered from square to squircle segments to maximise the confinement impact of the CFRP and BFRP in the core. The experimental results demonstrated that the moment capacity and deflection of CFRP and BFRP strengthened specimens were increased, respectively, and that the squircle cross-section assisted in preventing CFRP and BFRP debonding in the core. **Mohammd et al. (2022)** experimental study showed that CFRP-strengthening of beam-column joints delayed the formation of the plastic hinges, efficiently controlled the inelastic deformation at the critical plastic hinge locations, and significantly improved the seismic performance of the building**. Obaidat et al. (2019)**

conducted an experimental study on the behavior of repaired RC beam-column joints under cyclic loading using carbon fibre-reinforced plastics (CFRP) plates to study the behavior of repaired RC beam-column joints under cyclic loading with a variety of retrofitting schemes. Under cyclic loading, the specimen was tested to failure. All repaired joints have improved strength, approaching the beam-column joint's existing shear strength. The repaired joints had significantly higher strength-capacity than the reference joints. The studies done shows that the use of CFRP-plates significantly increased the load-carrying capacity of joints, while the mode of failure was changed from diagonal cracks to debonding of CFRP-plates in retrofitted joints. FRP as a strengthening material has the following advantages, such as quick application, short building time, lightweight, and corrosion resistant qualities, which increase the material's capabilities over other materials (**Wang et al. 2019, Mohanan et. al. 2016). Sakthimurugan et al. (2021)** conducted experimental analysis of beam column joint by using BFRP fabric for the retrofitting of damaged beam column joint. The 3 sided and 4-sided wrapping of BFRP enhanced the performance of beam column joint under static loading. **Abu Tahnat et al. (2018)** investigated the ductility behavior of R.C exterior joints strengthened by FRP using numerical analysis using commercial finite element-based software (ABAQUS). The developed F.E. model produced realistic and accurate results while capturing the joint's nonlinear complex behavior. The results show that wrapping a beam column joint with CFRP converts brittle failure to ductile failure. Stirrup’s continuity within the joint increased capacity and ductility in shear failure models.

2.1.3 Techniques for placings of FRP

In the experimental analysis done on beam column joint strengthened with CFRP. Use of Near Surface Mounted (NSM) CFRP composite strips along the column axis was less effective in improving load carrying capacity **(Elsanadedy et al. 2021).** The Externally Bonded Reinforcement on Grooves (EBROG) technique was used in strengthening beam column joint with FRP composite sheets. EBROG technique was c capable of eliminating surface debonding and compressive buckling failure of composite sheets **(Al-Rousan et al. 2021)**. EBROG technique enhanced seismic performance of the deficient beam-column joints in terms of load-carrying capacity, ductility, and energy dissipation **(Ilia and Mostofinejad 2019)**. When compared to the externally bonding technique (EBR), the near surface mounting technique has several

advantages: A wider bond surface induces better anchorage capability, it gives greater resistance to peeling-off, allowing a greater percentage of the tensile strength to be mobilised, no preparation work is necessary other than grooving, resulting in a shorter installation time **(Cruz JMS et al., (2002).** EBROG method changed the brittle shear failure mode into a flexural one at the beam column interface and it also enhanced the ultimate load and prevented debonding of CFRP sheets **(Singh et al. 2014)**

2.3 Gap Identified

The research gaps identified form the literature survey are as follows: -

1. Studies on the beam column joint with opening is limited
2. Effect of retrofitting with CFRP and BFRP on beam column joint with transverse beam opening is not studied.
3. Literature sources on numerical analysis of BFRP retrofitted beam column joint is very less

2.4 Objectives of the Study

The objectives of the study are as shown below:

1. To study the behaviour of CFRP and BFRP retrofitted beam-column joint with transverse web opening under axial load and reverse cyclic loading
2. To study the behaviour by varying opening size and distance from the joint
3. To study the effect of number of layers of CFRP and BFRP fabric on the behaviour of retrofitted beam column joints
4. To analyse the joint in terms of ductility, energy dissipation and stiffness
5. To compare the result of CFRP and BFRP retrofitting

2.5 Scope of the Study

The study is restricted to the following domains:

- Exterior beam-column joint
- Non-linear static analysis
- Analytical study using Ansys
- Design codes ACI 318M-02 and ACI 352R-02 for beam-column joint design
- Use of carbon fiber reinforced polymer and basalt fiber reinforced polymer

Chapter 3

Methodology

3.1 General

Exterior beam column joint with transverse beam opening structural model is used. Numerical investigation of structures offers an attractive technique of research due to low cost, quick results and ability to study several variables in detail. Therefore, a three-dimensional non-linear finite element joint model is built using commercial software Ansys. For conducting the analysis, the first step is the validation of Ansys software based on data from experimental analysis conducted by Sakthimurugan et al., (2021). For the fulfillment of the defined objectives, the steps followed are design of joint using ACI 352R-02 and ACI 318-2011, structural modelling, nonlinear static analysis, parametric study, development of force-displacement curve and comparative study. The parametric analysis improves understanding of the effect of CFRP and BFRP layer on beam column joints with different opening size and location on transverse side of beam. A comparison study based on ductility, energy dissipation, and stiffness degradation of CFRP and BFRP retrofitted joints and normal joints with opening and also provides an in-depth review of joint performance. The force-displacement curve created from the data can be utilized as a useful tool to compare the performance of both the normal beam column joint and the retrofitted joint. The methodology of the project is outlined as flow chart in the Figure 3.1 shown below.

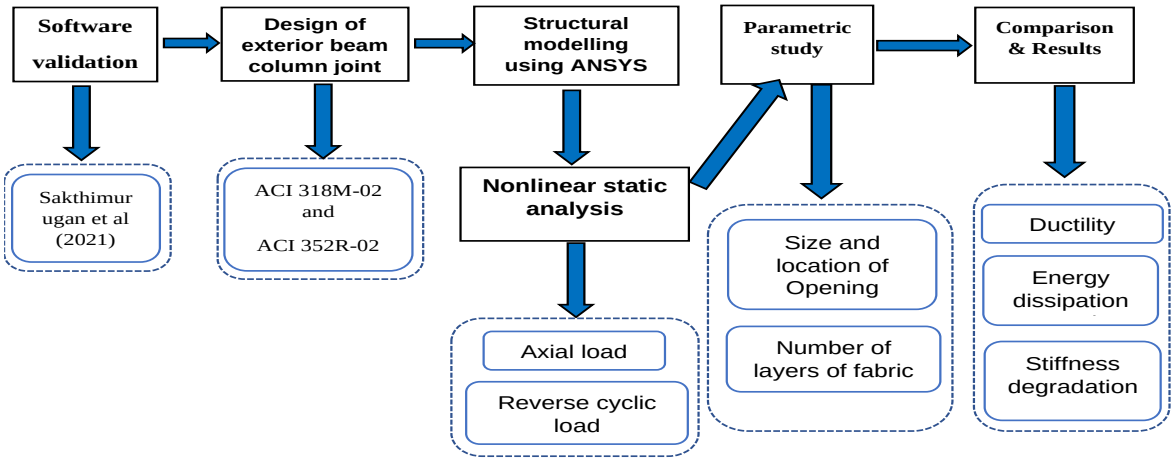

Figure 3.1 Flowchart of project methodology

3.2 Non- Linear Static Analysis

The exterior beam-column joint is subjected to nonlinear static analysis. A nonlinear analysis is one in which a nonlinear relationship exists between the applied forces and displacements. Geometrical nonlinearity, material, and touch can all cause nonlinear effects. As a result of these factors, the stiffness matrix is not constant during the load application. The design procedure for non-linear static analysis is as follows: -

Step 1: Defining material properties

Material properties can be defined by selecting the materials from the engineering data source, which contains a set of predefined materials or we can add new materials and input all properties of the respective materials to be used in the model. We will be defining the compressive strength of the concrete to be used, the stress-strain behavior of concrete, steel and FRP materials used, density of these materials, Elastic modulus and Poisson ratio, etc.

Step 2: Geometric Modelling

The geometry of the beam column joint is constructed in 'New DesignModeler Geometry'. Functions of designer modeler are similar to any CADD (Computer Aided Design and Drafting) software such as Solidwork, Creo etc., expect the Design Modeler is specially designed to create geometric models for use in ANSYS Workbench simulations. The geometry is drawn using the draw and modify tools.

Step 3: Result Analysis

The loading and boundary conditions is defined in the 'Model' section. In this structure, a constant axial load to be applied on top of the column which corresponds to the gravity load induced by the upper floors. And a cyclic load is to be applied at tip of beam to directly correlate the measured displacements of the joint to the inter-story drift of an entire frame. The load application is quasi-static with displacement control. It is intended to ensure that the applied reversed cyclic load was increased gradually in steps, neither too large nor too small. This is followed by an incremental load applied as displacement control.

Step 4: Comparison of Results

The required results are chosen under solution, which are total deformation, strain energy and force reaction in the direction of deformation are to be obtained. From the results, force displacement graph is plotted to give a clear idea on the performance of both the joints. It also helps to carry out a comparative study between the performance of normal beam column joint and retrofitted beam column joint.

3.3 Parametric Study

Parametric study is conducted to investigate the behavior of exterior beam column joint with transverse beam opening. when strengthened with CFRP and BFRP. The parameters in the study includes; Two shape of opening square and rectangle are provided and two locations of opening 150 and 300mm distance from column. Change in the CFRP and BFRP layer thickness from 1 to 3mm. Table 3.1 and Figure 3.2 shows the details of opening parameter.

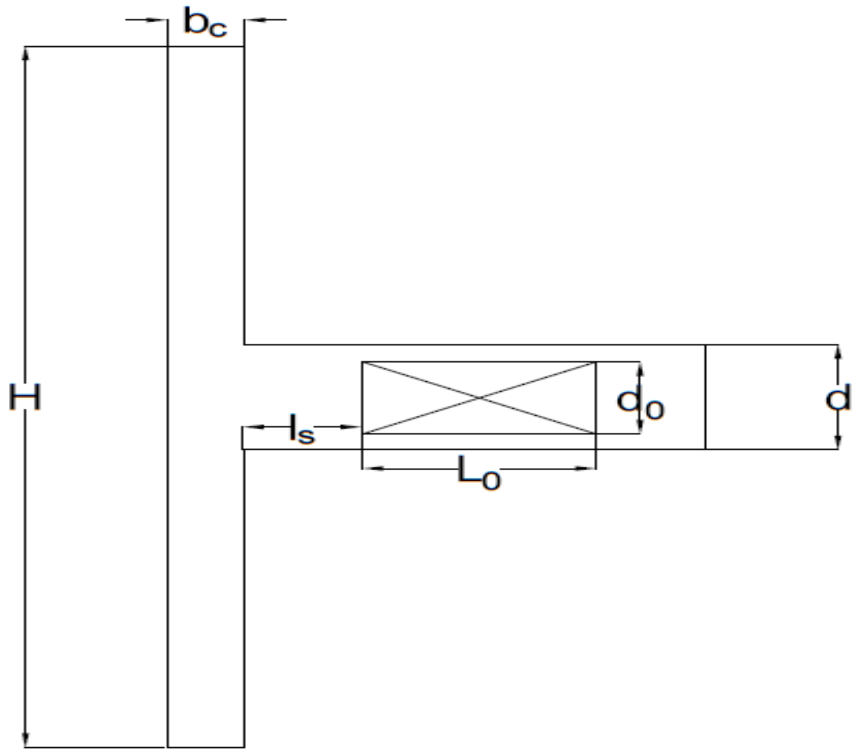

Figure 3.2 Details of opening parameter

Where;

- b_c = width of the column
- d = depth of the beam
- H = column height
- d_o = depth of the opening
- l_o = Length of the opening
- l_s = Spacing of opening from joint

Table 3.1 Details of opening parameter (Amin et al., 2017)

Shape of Opening	**Relative Opening Height to Beam Depth (d_s/d)**	**Relative Opening Length (l_s/d)**	**Opening proximity to support (l_o/d)**
Square	0.5	0.5	0.5
			1
Rectangle	0.5	1	0.5
			1

3.4 Comparative Study

The visualization module displays the analysis results. The output data required in the step module is obtained by this module. The deformation of the joint in the direction of the applied load verses time was obtained as the X-Y plot. Load was defined as a linear function of time in the obtained plot. Thus, the load verses displacement graph can be created by combining the data of load versus time and displacement versus time from the X-Y data. Load deformation graphs for retrofitted joint models were developed. The load displacement graph can be used to calculate the ductility, energy dissipation capacity, and stiffness degradation of joints. The results of the retrofitted joints' analyses were compared to those of the normal joints in order to comprehend the

improvement in structural performance of the CFRP and BFRP retrofitted beam column joint.

3.5 Design of Exterior Beam Column Joint

Exterior beam-column joint is designed using ACI 352R-02 and ACI 318M-02. ACI 352R-02 and ACI 318M-02 are used to design the outside beam-column joint. Only structures made of normal weight concrete with a compressive strength of less than 100 MPa are covered by these codal recommendations. The Type 2 connection is selected for joint design in this investigation. The following are the steps of developing a beam column joint:

Step 1: Determine the material properties and the beam-column joint dimension

The material properties of the beam-column joint that is designed based on the analysis are shown in Table 3.2 are as follows:

Table 3.2 Material properties of the beam-column joint

PARAMETER	STEEL	CONCRETE
Density (kg/m3)	7800	29250
Young ‘modulus (MPa)	200000	25000
Poisson’s ratio	0.30	0.2

Dimensions of exterior beam column joint are as follows:

Column - cross section of 150 mm x 300 mm and height of 2000 mm

Beam - 150 mm x 300 mm cross section and length of 900 mm

Step 2: Calculate the amount of reinforcement

Section 10.9.1 of ACI 318-2011 specifies that the area of longitudinal reinforcement for non-composite compression members should not be less than 0.01 times the gross section of the column and should not be greater than 0.08 times the gross section of the column. In addition, according to section 10.9.2 of the same, the minimum number of longitudinal bars for rectangular or circular sections should be four. Section 10.5.1 of ACI 318-2011 requires beam reinforcement as shown in equation Eq. 3.1. In Eq. 3.2, Asmin represents the minimum area of reinforcement, fc' represents the compressive strength of concrete, bw represents the web width of the beam, d represents the depth

of the beam, fy represents the yield strength of steel, and A_s represents the area of steel reinforcement. Section 7.10.5.1 of ACI 318-2011 requires at least 8mm diameter ties for longitudinal bars of 30mm or less.

Minimum reinforcement, $A_{smin} = (3\sqrt{f_c'}b_w d)/f_y$ Eq. 3.1

$= (3*\sqrt{30}*150*300)/415$

$= 1781\ mm^2$

Area of steel reinforcement, $A_{st} \leq (200bwd) / f_y$ Eq. 3.2

$\leq (200*150*300)/415$

$\leq 21687\ mm^2$

Step 3: Calculate the design shear force of beam-column joint

The magnitude of the shear force of the joint (Vu) is calculated by finding the difference in the amount of tension and compression to the horizontal shear force that works on the column as given by equation Eq. 3.3. where Cs and Ts are the beam compression and tension forces given by equations Eq. 3.4 and Eq.3.5, Vc is the horizontal shear force on the column, is the stress multiplier for longitudinal reinforcement and is equal to 1.25, fy is the yield strength of steel, The equation Eq. 3.8 gives the column shear force. where Mprb is the beam moment, h is the column height, As is the sum of top and bottom beam longitudinal reinforcement (Eq. 3.7), d is the beam depth, fc' is the concrete compressive strength, and b is the beam breadth. The shear force of the joint is to be calculated using all of the above equations and appropriate values.

Design shear force of the joint, $Vu = (Ts + Cs) – Vc$ Eq. 3.3

Sum of top and bottom beam longitudinal reinforcement,

$A_s = A_{s1} + A_{s2}$

$= 2*0.78*122+2*0.78*162$

$= 628.314\ mm^2$

Beam compression force, $C_s = \alpha\ f_y\ A_s$ Eq. 3.4

$= 1.25*415*302.64$

$= 156.99$ KN

Beam tension, $T_s = \alpha\ f_y\ A_s$ Eq.3.5

$= 1.25*415*402.124$

$=208.6$ kN

$$a = (AS\ \alpha\ f_y)\ /(0.85fc'b) \qquad \text{Eq.3.6}$$

$$= (628.314*1.25*415)/(0.85*30*150)$$

$$= 85.215 \text{ mm}$$

$$\text{Beam moment, } M_{prb} = 2\ As\ \alpha\ fy\ (d- a/2) \qquad \text{Eq. 3.7}$$

$$= 2*628.314*1.25*415*(300-85.21)$$

$$=140 \text{ kNm}$$

$$\text{Horizontal shear on column, } V_c = M_{prb} / h \qquad \text{Eq. 3.8}$$

$$= (140/2)$$

$$=70 \text{ kN}$$

$$\text{Design shear force of the joint, } V_u = (T_s + C_s) – V_c$$

$$= 252 \text{ kN}$$

Step 4: Calculate the concrete shear capacity of joint

Current building codes in high seismic zones require the design of reinforced beam-column joints to take joint shear failure into account. This is due to the observation that joint shear failure occurs prior to beam or column flexural yielding. Eq. 3.9 is used to calculate the concrete shear capacity (Vc).

$$\text{Concrete shear capacity, } V_{cs} = 0.2905\sqrt{f_c'}\sqrt{(1+ 0.2903\ N_u/A_g)} \qquad \text{Eq. 3.9}$$

$$= 0.2905\sqrt{30'}\sqrt{(1+ 0.2903\ *100000/(150*300)\ )}$$

$$= 130 \text{ kN}$$

where Nu denotes the axial force acting on the column and Ag denotes the gross column area The concrete shear capacity of the joint must be determined. If the axial compressive stress in the column Nu/Ag is less than 0.12 fc', the contribution of concrete shear resistance should be ignored.

Step 5: Calculate the joint shear strength

The horizontal shear in the joint must be checked independently in each direction in connections with beams framing in from two perpendicular directions. The design shear force Vu is computed on a horizontal plane at the joint's mid-height by taking into account the shear forces on the joint's boundaries as well as the normal tension and compression forces in the members framing the joint. Eq. 3.11 is used to calculate the joint shear strength (Vn). Eq. 3.10 should also be met.

$$\varphi Vn \geq Vu \qquad \text{Eq. 3.10}$$

$$Vn=0.083\gamma\sqrt{fc'}bjhc \quad \text{Eq. 3.11}$$

$$bj = (bb + bc)/2 \quad \text{Eq. 3.12}$$

Effective width of joint transverse to the direction of shear,

$$b_j = (b_c + b_b)/2$$

$$= (300+300)/2$$

$$= 300 \text{ mm}$$

Joint shear strength, $V_n=0.083\gamma\sqrt{f_c'}b_jh_c$

$$= 0.083*20*\sqrt{30}*300*1500$$

$$= 5455 \text{ kN}$$

$$\varphi V_n \geq V_u$$

$$0.85* 5455 \geq 252 \text{ kN}$$

where is the strength reduction factor and equals 0.85, is the shear strength factor reflecting joint confinement by lateral members and equals 20, bj is the effective width of joint transverse to shear (Eq. 3.12), hc is the full depth of column, bb is the web-width of beam, bc is the core dimension of tied column, and m is the slope to define the effective width of joint transverse to shear. The joint shear strength must be determined. The design philosophy embodied in Eq. 3.12 is that the joint can resist the specified shear forces if the concrete within the joint is adequately confined during anticipated earthquake-induced loading and displacement demands.

Step 6: Design shear force of joint stirrup

The amount of design shear force that must be resisted by stirrups Vs is given by the equation Eq. 3.13 and is to be obtained.

$$\text{Design shear force, } V_s = V_u - V_c \quad \text{Eq. 3.13}$$

$$= 124 \text{ kN}$$

Chapter 4

Validation

The Ansys software was validated using the results published by Sakthimurugan. et al., (2021). Experimental analysis to study the behaviour of beam-column joint strengthened using BFRP fabric under static load is presented in this work. In addition to the 3 appropriately detailed control specimen, the programme includes testing 8 specimens separated into three groups based on the BFRP wrapping. BFRP is provided in the form of 3 side wrapping in beam one and two layer and also 4 side wrapping with one layer. Failure criteria such as ultimate capacity, mode of failure, Variation in dissipation energy and developed ultimate strain in reinforcing steel and BFRP were studied and compared for each group of control and BFRP-enhanced specimens.

Ansys software was used to simulate the experimentally tested model. The model was built in the same manner as the experimental setup and is composed of M20 grade concrete. The reinforcement details of the beam-column joint used in the study are shown in figure 4.1. The segment comprises a 450 mm long extruded beam and cross-sectional dimensions of 100 x 120 mm. At its mid-height, this beam was attached to a column. The column's cross-section measured 200 x 100 mm. The columns' entire length was 0.6 m, divided into two equal portions, bottom and upper. High tensile steel was used for the beam's upper and lower reinforcement, as well as the column's primary longitudinal steel reinforcement. The beam is reinforced with four bars of 8 mm diameter. On the other hand, the column was reinforced with four bars of 16 mm diameter at each corner of the column cross-section. The stirrups for both beam and column weremild steel bars of 6 mm diameter and spaced every 100 mm and 125 mm for the beam and the column, respectively. The longitudinal reinforcement for the beam and columns was deformed bars with a yield strength of 500 MPa, while the stirrups were conventional mild steel with a yield value of 415 MPa.

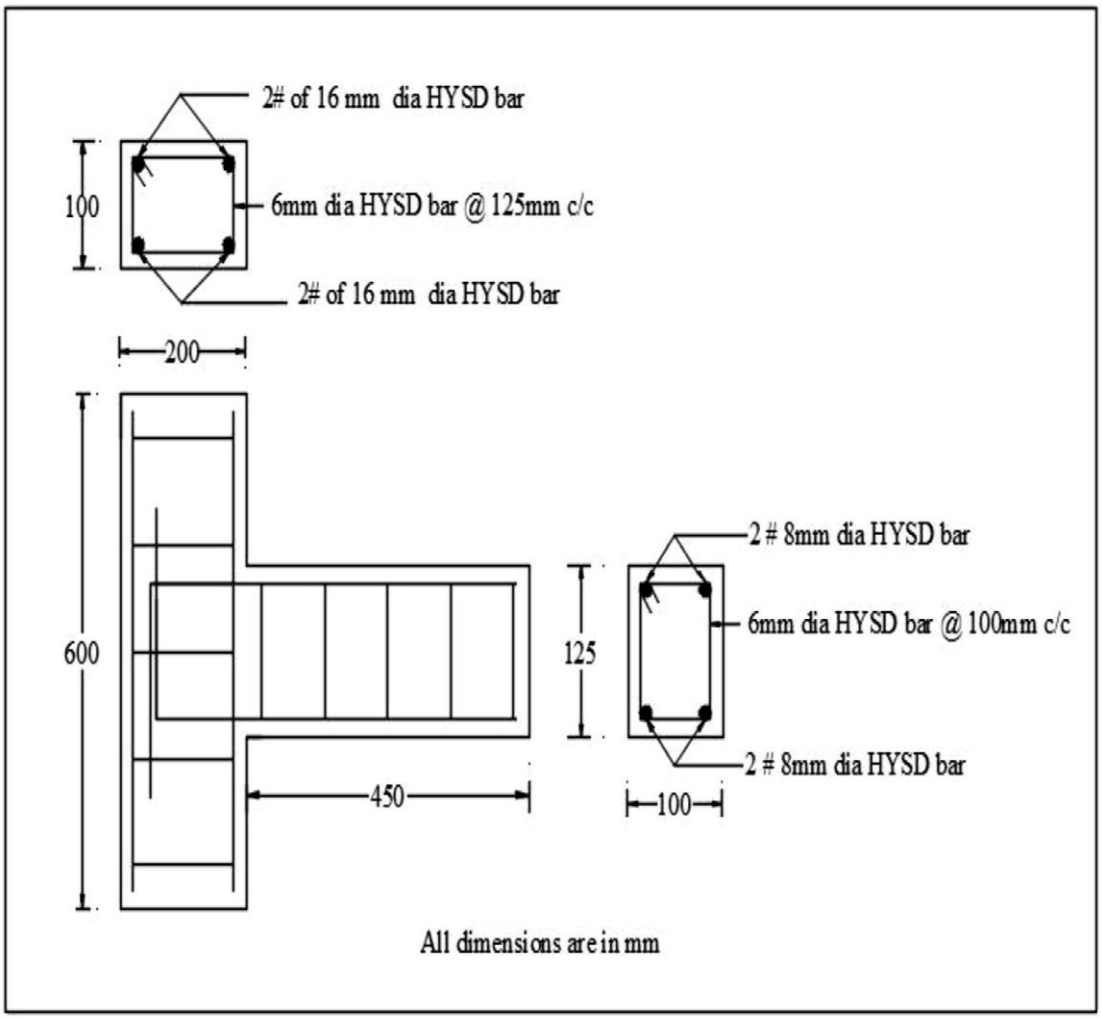

Figure 4.1 Reinforcement details for beam column joint

(Source: Sakthimurugan et al., 2021)

Each end of column in the specimens were considered hinged. Before loading the beam, a compression load of 25 kN was given to the column to simulate the load in a genuine structure. During the loading phase, the column load was kept constant. As a result, the beam was loaded to failure in stages.

The joint model developed in Ansys is shown in figure 4.2. Meshed model with mesh size of 40 is shown in figure 4.3. Loading stage of beam column joint is shown in figure 4.4. and the deformed model of joint after loading stage is shown in figure 4.5

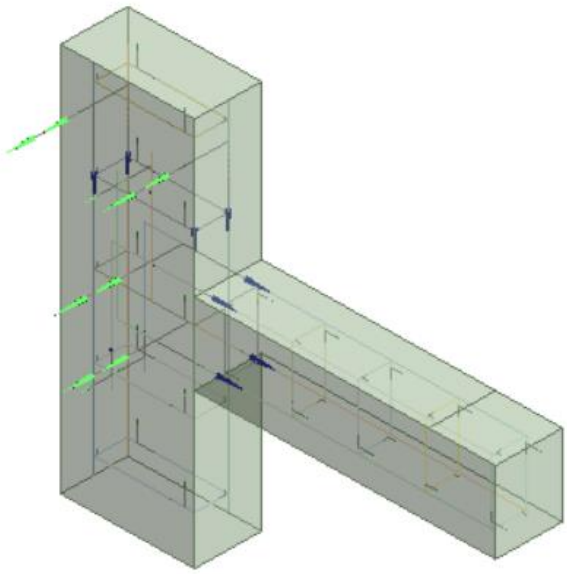

Figure 4.2 Beam column joint model in Ansys

(Source: Sakthimurugan et al., 2021)

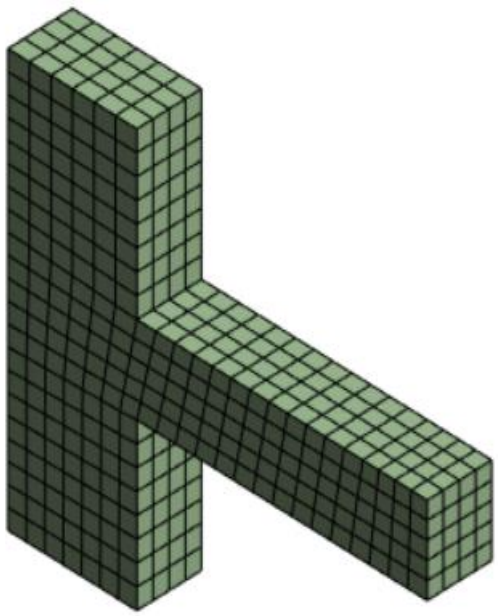

Figure 4.3 Meshed model in Ansys

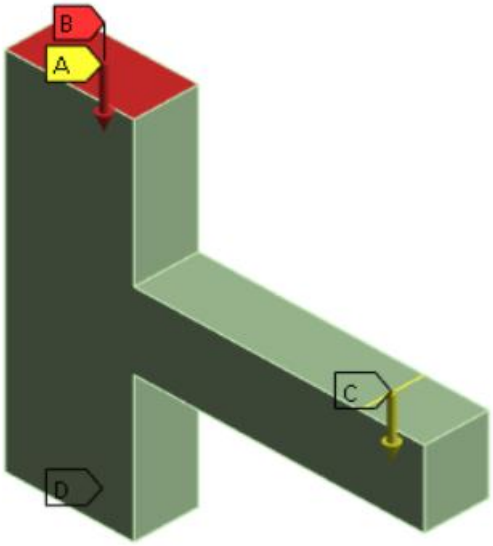

Figure 4.4 Loading Model in Ansys

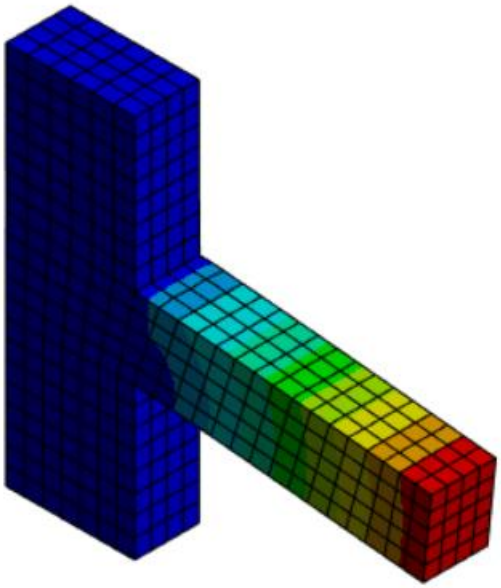

Figure 4.5 Deformed Model

Figure 4.6 shows the graph comparing the reported experimental results and finite element results obtained. The finite element analysis results of the exterior connection specimen with 40 mm mesh sizes are studied in this work to analyze the mesh size sensitivity of the numerical model. The graphs show that the finite element findings are very close to the experimental data.

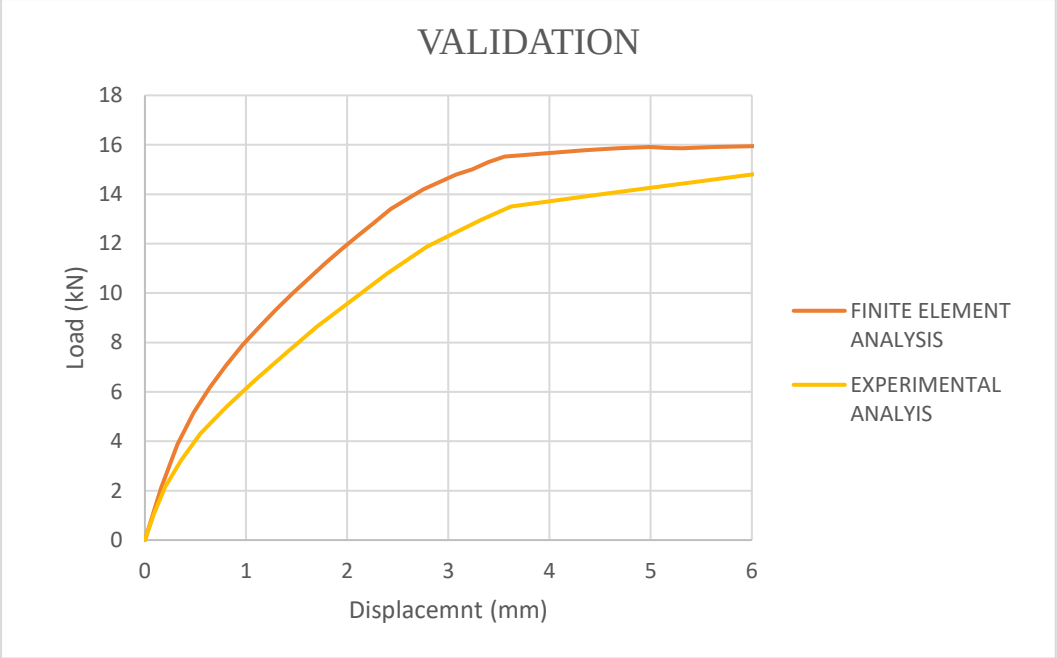

Figure 4.6 Comparison of Experimental and finite element analysis

Parity Curve is plotted for the ultimate load and displacement within a 10% variation as shown in fig 4.7 and 4.8

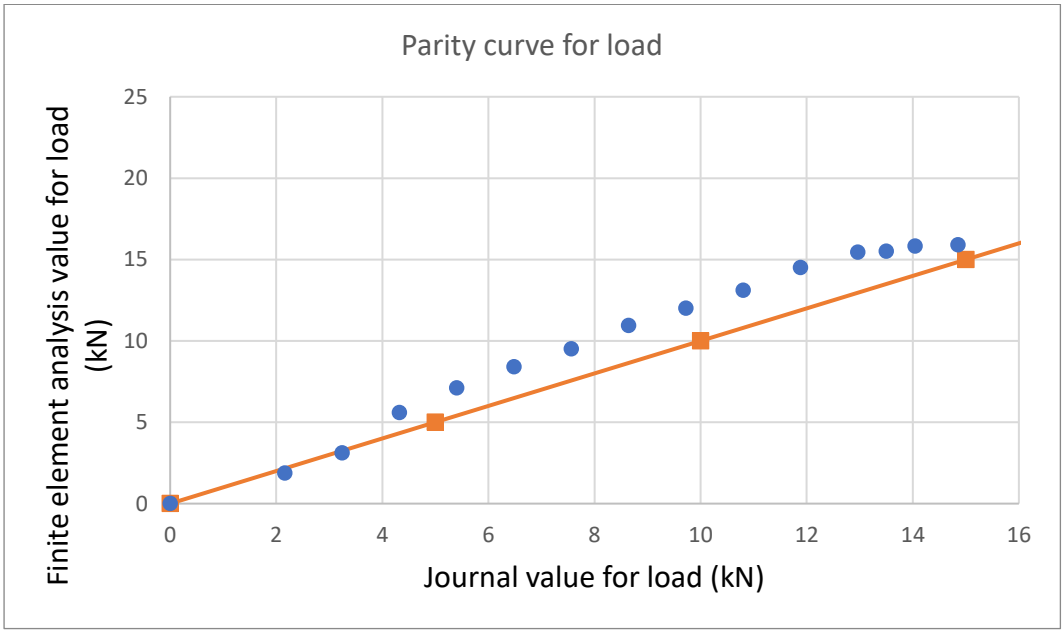

Figure 4.7 Parity Curve for load

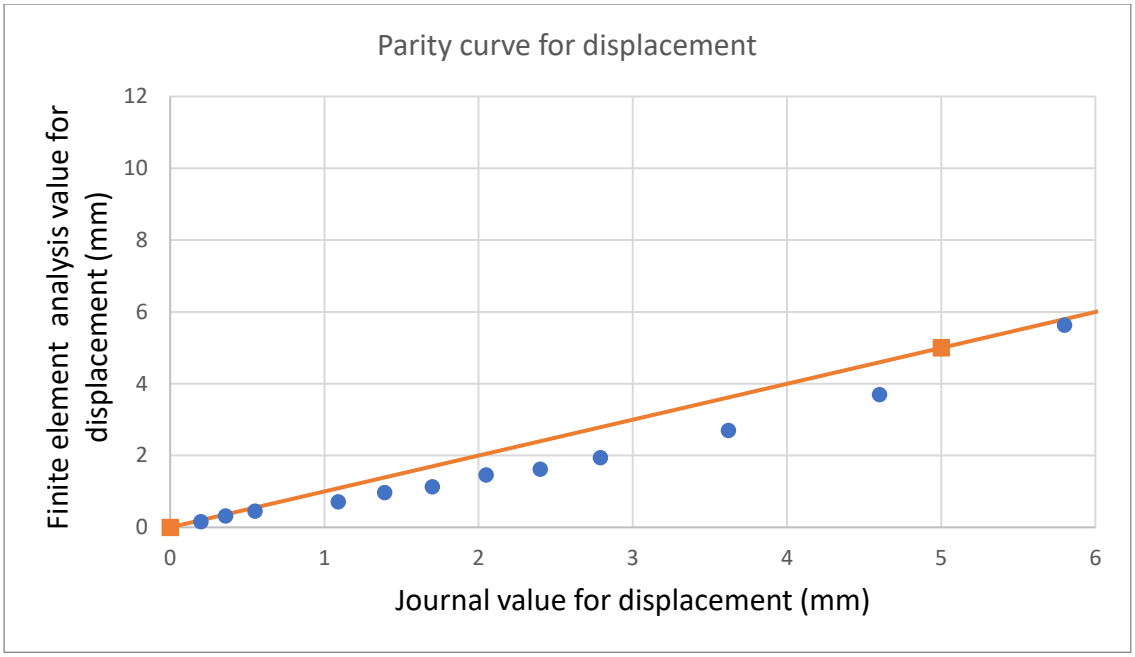

Figure 4.8 Parity Curve for displacement

The ultimate load value and displacement value from the numerical analysis and from the experimental analysis are tabulated below in Table 4.1. A variation of 7.1% and 7.7% are observed in ultimate load and displacement values respectively for mesh size 40. Since the difference is less than 10% the software and model can be used for analysis.

Table 4.1 Comparison of ultimate load and displacement of joint

Parameters	From experimental analysis	Mesh size= 40mm	Error %
Ultimate load (KN)	14.85	15.9	7.1%
Displacement	6.1	5.63	7.7%

Although the impacts of mesh size and strain localization in the numerical model are within the margins of error expected for most numerical simulations based on plasticity models, there are minor changes in peak lateral loads and displacements. The minor variances could be attributed to variations in the unknown assumptions used in establishing material attributes and the interaction between reinforcement and concrete.

Chapter 5

Numerical Analysis of Beam Column Joint

5.1 Modelling in Ansys

The exterior beam column joint is developed in Ansys and is shown in figure 7.1. The structural dimensions are summarized in having a vertical column with a cross section of 200 mm x 200 mm intersecting a horizontal beam with a 150 mm x 300 mm cross section. The height of the specimen is 2000 mm and the beams extend by 900 mm before and after the connection. The longitudinal reinforcement of the column is 4 number of 16 mm diameter rebars and the shear reinforcement is 8 mm diameter stirrups with a spacing of 110mm given in figure 5.1. The beam bottom steel reinforcement consists of 3 number of 16 mm diameter rebars, and top reinforcement consist of 2 bar of 12 mm diameter with shear reinforcement of 8 mm diameter stirrups with a spacing of 100 mm. Clear cover of 40mm is provided for beams and column.

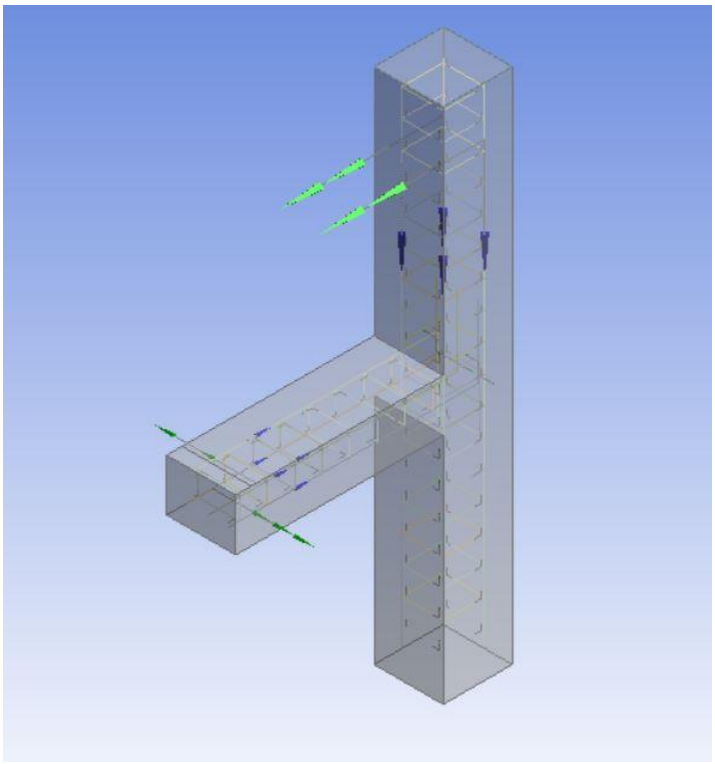

Figure 5.1 Reinforcement details of model developed in Ansys

Total of 25 different models are made for the comparison. That include different variation in FRP provided. Twenty-five models comprise of Normal beam column joint, 4 models with different shape and location of transverse beam opening and 20 models with respective unidirectional CFRP and BFRP wrapping with 2 layers starting with a layer of 1mm thickness. The details of models are shown in Table 5.1.

Table 5.1. Details of models

Models	No of CFRP Layers	No of BFRP Layers	Shape and Size of Opening	Opening proximity to support
NC	-	-	-	-
NS150	-	-	Square (150x150mm)	150
NS300	-	-	Square (150x150mm)	300
NR150	-	-	Rectangle (300x150mm)	150
NR300	-	-	Rectangle (300x150mm)	300
CF1	1	-	-	-
CF2	2	-	-	-
BF1	-	1	-	-
BF2	-	2	-	-
CF1S150	1	-	Square (150x150mm)	150
CF2S150	2	-	Square (150x150mm)	150
BF1S150	-	1	Square (150x150mm)	150
BF2S150	-	2	Square (150x150mm)	150
CF1S300	1	-	Square (150x150mm)	300
CF2S300	2	-	Square (150x150mm)	300
BF1S300	-	1	Square (150x150mm)	300
BF2S300	-	2	Square (150x150mm)	300
CF1R150	1	-	Rectangle (300x150mm)	150

CF2R150	2	-	Rectangle (300x150mm)	150
BF1R150	-	1	Rectangle (300x150mm)	150
BF2R150	-	2	Rectangle (300x150mm)	150
CF1R300	1	-	Rectangle (300x150mm)	300
CF2R300	2	-	Rectangle (300x150mm)	300
BF1R300	-	1	Rectangle (300x150mm)	300
BF2R300	-	2	Rectangle (300x150mm)	300

5.2 Elements Used in Ansys

Concrete had been modelled using SOLID65 element. Reinforcing bar has been modelled using LINK180 element. Contact surface has been modelled as bonded condition.

5.2.1 SOLID65

SOLID65 is a 3-D modelling element used in Ansys software for solids with or without reinforcing bars (rebar). The solid has the ability to crack in tension and crush in compression. In concrete applications, for example, the element's solid capacity can be used to represent the concrete, while the rebar capability can be utilised to model reinforcing behaviour. The element is defined by eight nodes, each of which has three degrees of freedom: translations in the nodal x, y, and z directions. It is possible to declare up to three different rebar requirements. The consideration of nonlinear material properties is the most essential component of this part. Concrete has the ability to crack (in three orthogonal directions), crush, distort, and creep.

5.2.2 LINK180

LINK180 is a three-dimensional spar that may be used in a range of engineering applications. The element can be used to simulate trusses, sagging cables, linkages, springs, and other structures. The element is a uniaxial tension-compression element with three degrees of freedom at each node: nodal x, y, and z translations. There are tension-only (cable) and compression-only (gap) alternatives available. No bending of the element is considered, as in a pin-jointed structure. Plasticity, creep, rotation,

significant deflection, and large strain are all supported. LINK180 includes stress-stiffness terms by default in any study that contains large-deflection effects. The following properties are supported: elasticity, isotropic hardening plasticity, kinematic hardening plasticity, Hill anisotropic plasticity, Nonlinear hardening plasticity, and creep.

5.3 Material Properties

5.3.1 Concrete

Concrete material property is defined using command function in ANSYS. The material property of M30 concrete used for the analysis is shown in Table 5.2. The Stress-Strain behaviour of M30 concrete used in software is listed in Table 5.3.

Table 5.2 Material properties for concrete

Material Property	**CONCRETE**
Density (Kg/m3)	2400
Characteristic compressive strength (MPa)	30
Elastic modulus (MPa)	29250
Poisson Ratio	0.2

Table 5.3 Stress-Strain behaviour of concrete

Yield Stress	Inelastic strain
2.925	0.0001
5.7	0.0002
8.325	0.0003
10.8	0.0004
13.125	0.0005
15.3	0.0006
17.325	0.0007
19.2	0.0008
20.925	0.0009
22.5	0.001
25.2	0.0012
28.125	0.0015

28.8	0.0016
29.7	0.0018
29.925	0.0019
30	0.002
30	0.0024
30	0.0026
30	0.0028
30	0.0031
30	0.0033
30	0.0035

5.3.2 Reinforcing Steel

Steel reinforcement material property is defined using command function in ANSYS. Steel reinforcement of tensile strength 415MPa is also used for providing reinforcement bars and stirrups, listed in Table 5.4. The reinforcement was modelled using isotropic behaviour. As plastic straining occurs, the yield surface changes size uniformly in all directions, causing the yield stress to increase (or decrease) in all stress directions.

Table 5.4 Properties of reinforcement for the joint

Bar Diameter (mm)	**Cross sectional area (mm^2)**	**Yield strength (MPa)**
16	200.96	415
12	113.04	415
8	50.24	415

5.3.3 Modelling of FRP

The beam-column joint model is strengthened using unidirectional CFRP and BFRP Fabric. The fiber behaviour is linear elastic up to failure with rupture failure. Figure 5.2 shows the model of exterior beam column joint retrofitted with FRP fabric. Figure 5.3 (a) and (b) shows the model of exterior beam column with square and rectangular transverse beam opening retrofitted with FRP fabric. The mechanical properties for the CFRP sheet and BFRP fabric are listed as in table 5.5 and 5.6.

Table 5.5 Properties of CFRP fabric (Source: Sabara. et al., 2018)

Material Property	**CFRP**
Density (Kg/m3)	1740
Elastic modulus (GPa)	230
Poisson Ratio	0.2
Tensile strength (MPa)	3790
Thickness (mm)	1

Table 5.6 Properties of BFRP fabric (Source: Sakthimurugan. et al., 2021)

Material Property	**BFRP**
Density (Kg/mm3)	2660
Elastic modulus (MPa)	89
Poisson Ratio	0.26
Tensile strength (MPa)	4200
Thickness (mm)	1

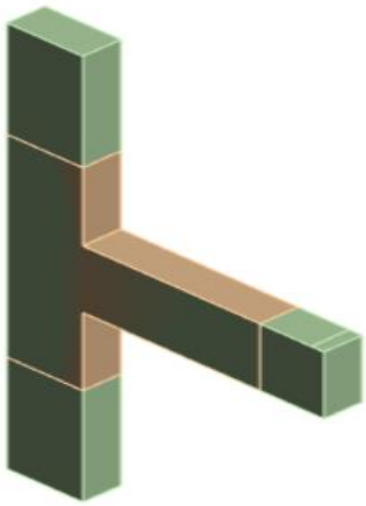

Figure 5.2 Model of exterior beam column joint retrofitted with FRP

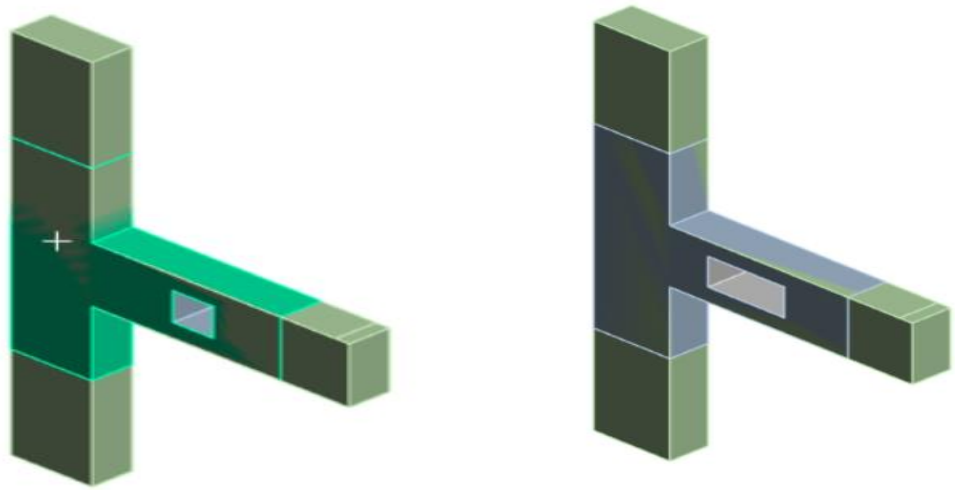

(a) (b)

Figure 5.3 FRP retrofitted beam column joint with opening (a) Square (b) rectangle

5.4 Loading and Boundary Conditions

The column is applied with a constant axial load initially at the top. A cyclic load is then provided at the beam's tip to control displacement. The top end of the column is restrained by a stiff surface, allowing it to behave like a pin, while the bottom end is restrained by a rigid surface, allowing it to behave like a fixed end. The connection at the top prevented the column's lateral displacement, but it was free to rotate and extend. The loading and boundary condition of joint is shown in figure 5.4 respectively.

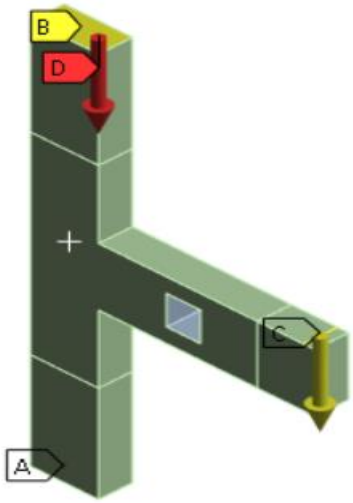

Figure 5.4 Loading and boundary conditions of joint in Ansys

5.5 Mesh Arrangement

Mesh size is a important aspect for any Finite element analysis. Since it splits complex geometries into simple parts that can be employed as different local approximations of the wider domain. A model's mesh arrangement affects the simulation's accuracy, convergence, and speed. The meshing method takes up a large amount of time while obtaining simulation results. The faster and more exact the answer, the better and more automated the meshing tools. Figures 5.5 and 5.6 show a meshed model of a normal joint and a retrofitted joint. A mesh size of 40 mm is used in this study.

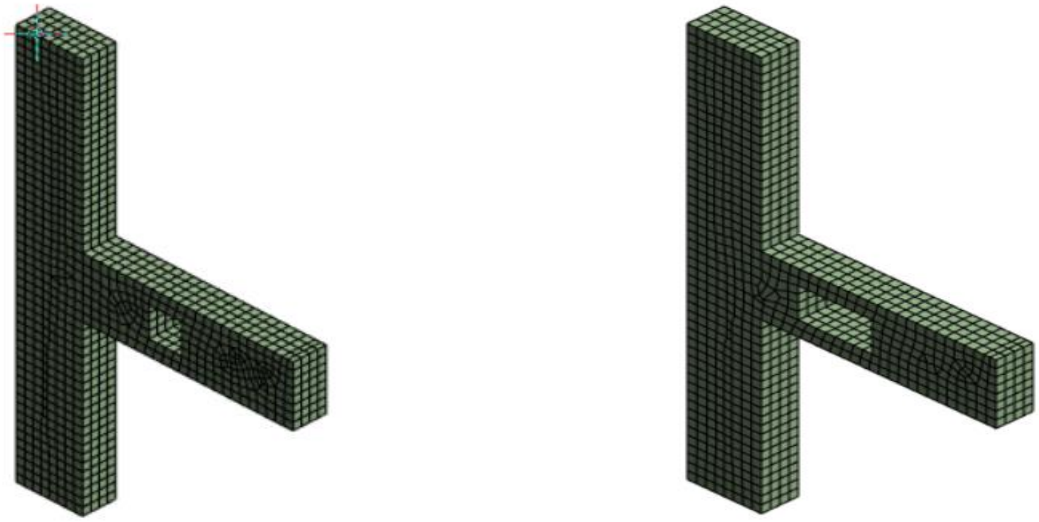

(a) (b)

Figure 5.5 Meshed model of normal joint with (a) Square (b) Rectangular opening

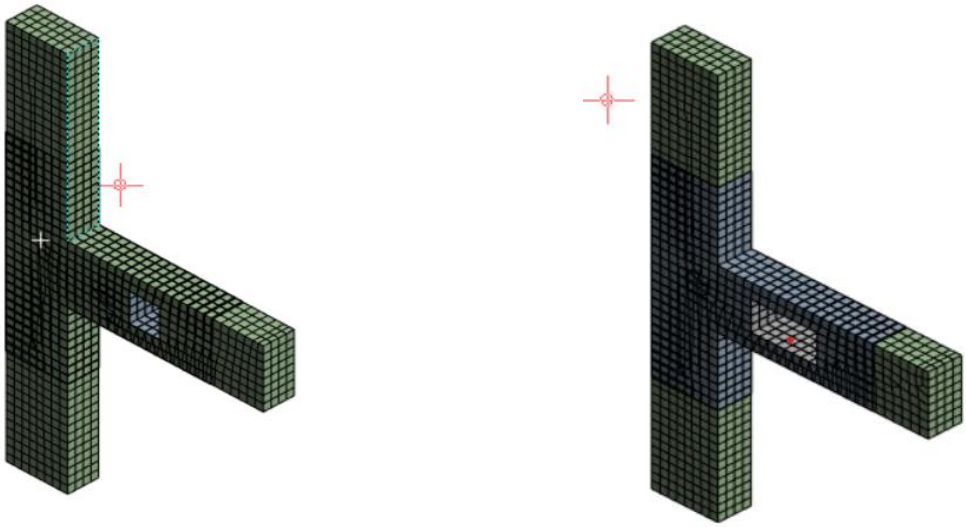

(a) (b)

Figure 5.6 Meshed model of FRP retrofitted joint with (a) Square (b) Rectangular opening

Chapter 6

Result and Discussions

6.1 General

The numerical analysis on retrofitted beam column joint with transverse beam opening was performed to evaluate the improvement in load carrying capability of retrofitted joint with CFRP and BFRP, it is then compared to that of a normal joint. The effect of factors, namely change in size, location of opening in beam and the change in layer thickness of CFRP and BFRP was explored, and the results are discussed in the following sections.

6.2 Effect of Opening on Normal Beam Column Joint

To investigate the effect of opening on the performance of beam column joints, study on beam column joints with two shape of transverse beam opening square (150mm x150mm) and rectangular (300mm x150mm) at a distance of 150mm and 300mm from joint were numerically analyzed, and the results were compared to the load carrying capacity of a normal joint. Deformed model of beam column joint with different shape of opening and distance from joint is shown in figure 6.1 and figure 6.2 represents the load displacement curve for beam column joint with transverse beam opening at a distance of 150mm and 300mm from joint. According to the graph, Presence of opening and proximity to support decreases the load carrying capacity of the joint compared to Normal beam column joint. The load carrying capacity of beam column junction with rectangular transverse beam opening at a distance of 150mm from support (NR150) showed the lowest strength compared to other beam column joint with opening. The decrease in the load carrying capacity of beam column joint with square opening NS150 and NS300 were 29.2% and 16.8%. Similarly, the load carrying capacity of beam column joint with rectangular opening NR150 and NR300 were 43.5% and 37.3% for opening at a distance of 150mm and 300mm from joint. Figure 6.3 shows the efficiency-displacement factor curve for beam column joint with different transverse beam opening. The variation of efficiency and load factor curve is similar in all three cases and hence the result is verified.

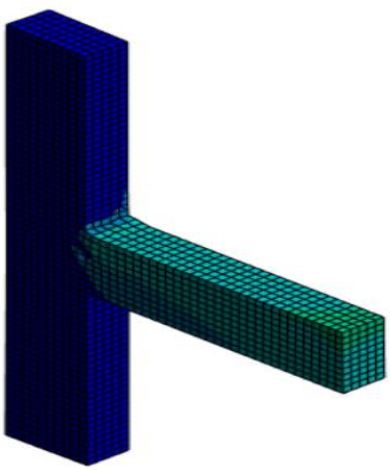

(a) NC

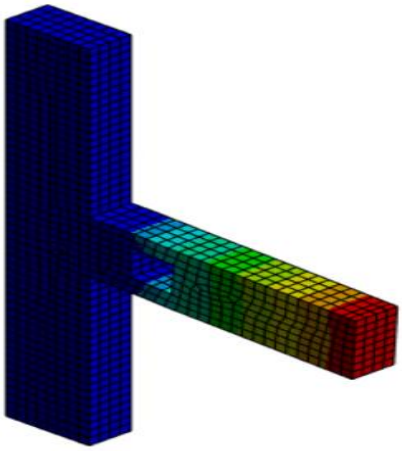

(b) NS150

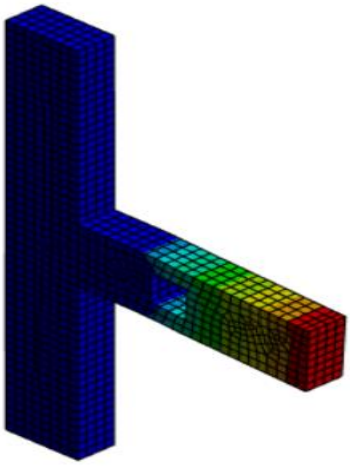

(c) NS300

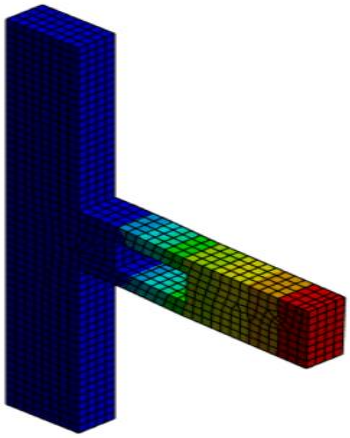

(d) NR150

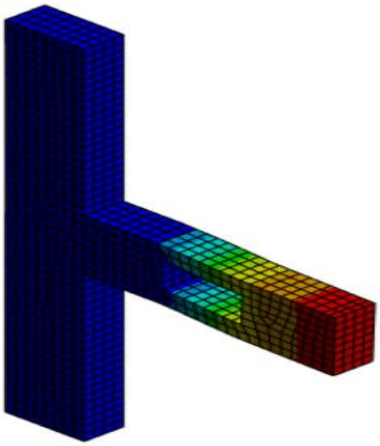

(e)NR300

Figure 6.1 Deformed model with different transverse beam opening: (a) NC, (b) NS150 (c) NS300 (d) NR150 and (d) NR300

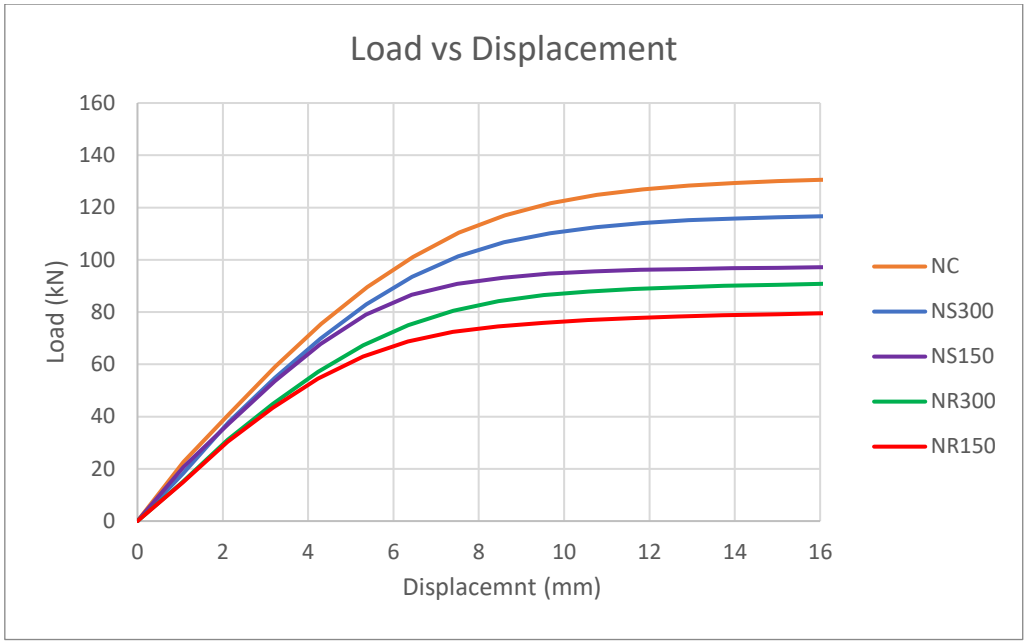

Figure 6.2 Load-displacement curve of joint with different transverse beam opening

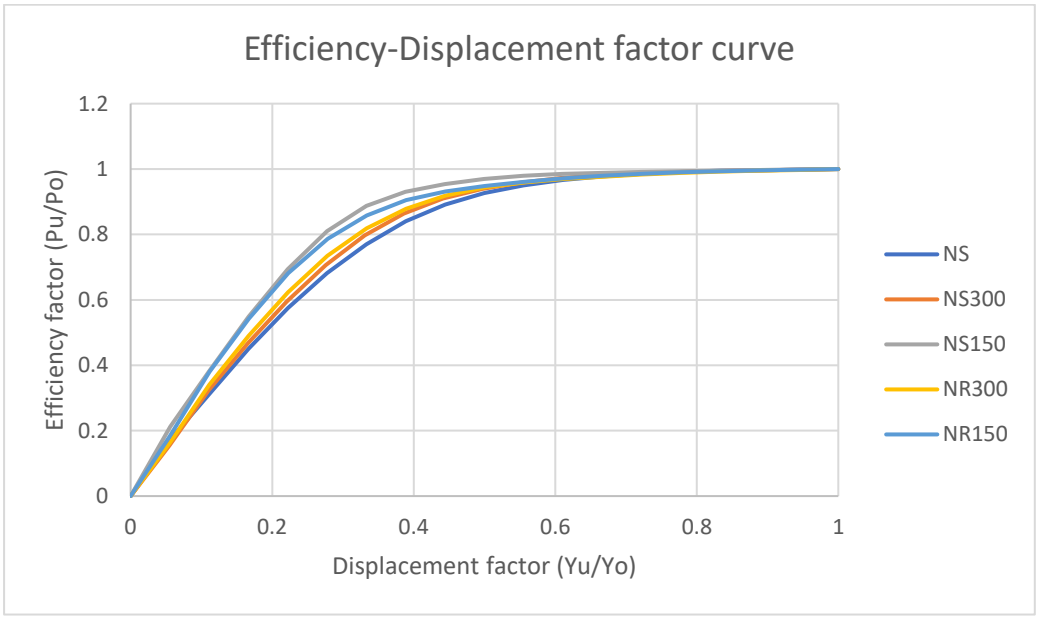

Figure 6.3 Efficiency-displacement of joint with different transverse beam opening

6.3 Effect of CFRP and BFRP on Normal Beam Column Joint

To investigate the effect of CFRP and BFRP on the performance of beam column joints, beam column joints is retrofitted CFRP and BFRP fabrics. The thickness of 1 and 2mm are used for both FRP and the models are analyzed and the results were compared to the load carrying capacity of a normal joint. Deformed model of

retrofitted joint with different FRP is shown in figure 6.4 and figure 6.5 represents the load displacement curve for beam column joint retrofitted with 1 and 2 layers of CFRP and BFRP and that of a normal joint. According to the graph, Use of FRP fabric increases the load carrying capacity of the joint more than Normal beam column joint. The load carrying capacity of a CFRP retrofitted beam column joints was greater than that of BFRP. The load carrying capacity increased with thickness of fabric. The improvement in the load carrying capacity of retrofitted beam column joint models CF1, CF2, BF1 and BF2 were 69.5%, 99%,46.7 and 89.7 % higher than that of the normal beam column joint (NS). Figure 6.6 shows the efficiency-displacement factor curve for retrofitted joint with different FRP combinations. The variation of efficiency and load factor curve is similar in all three cases and hence the result is verified.

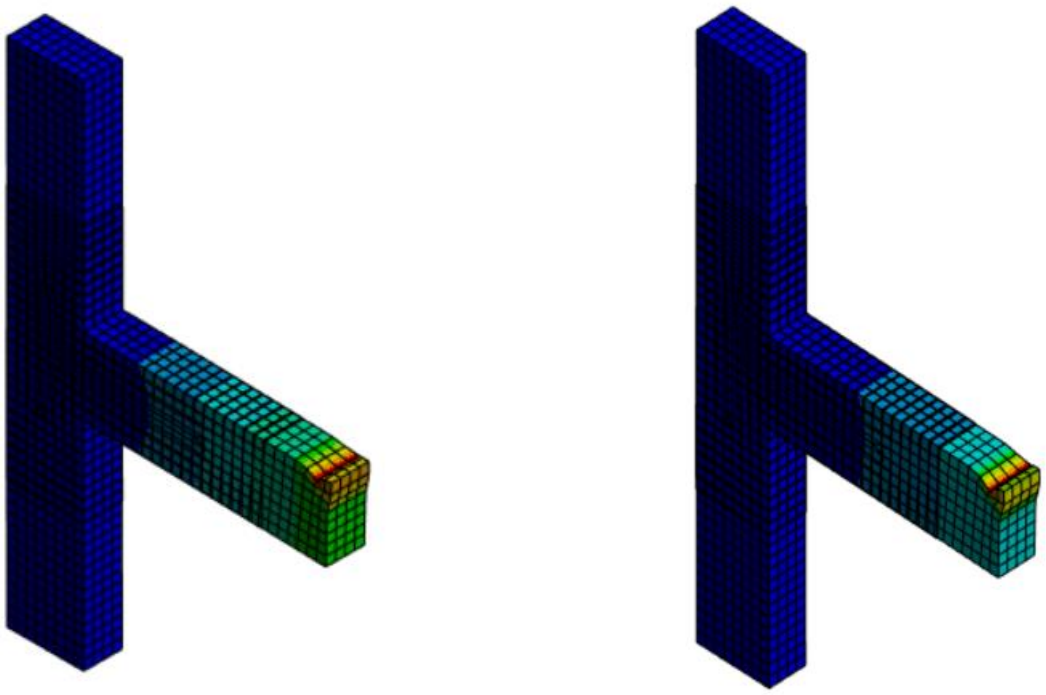

(a) CF1 (b) CF2

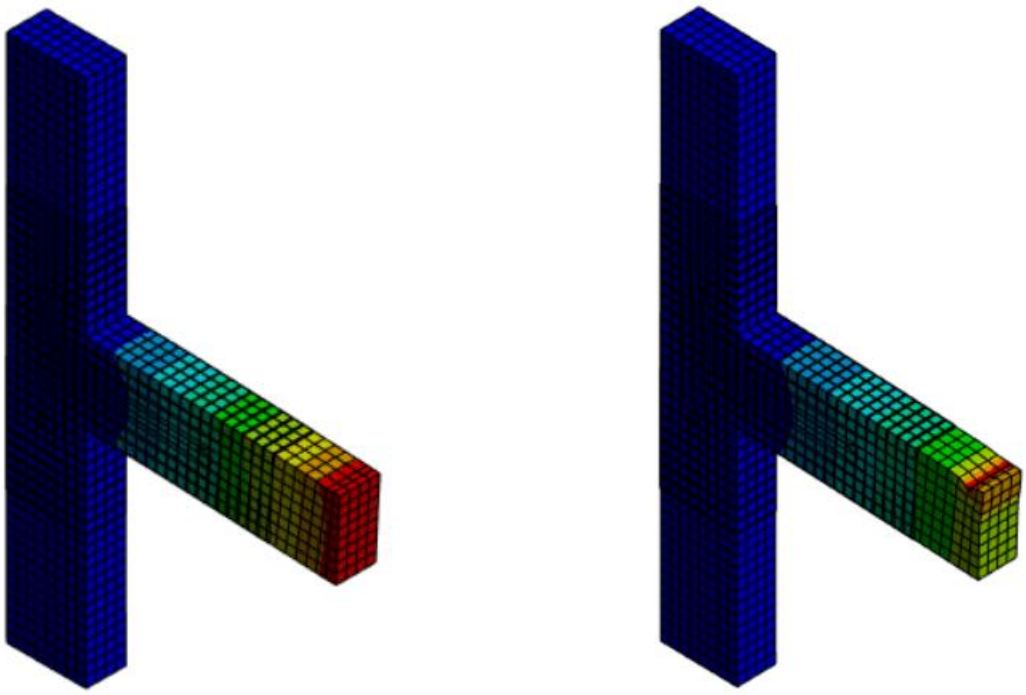

(a) BF1 (b) BF2

Figure 6.4 Deformed model of CFRP and BFRP retrofitted joint:(a) CF1 (b) CF2 (c) BF1 and (d) BF2

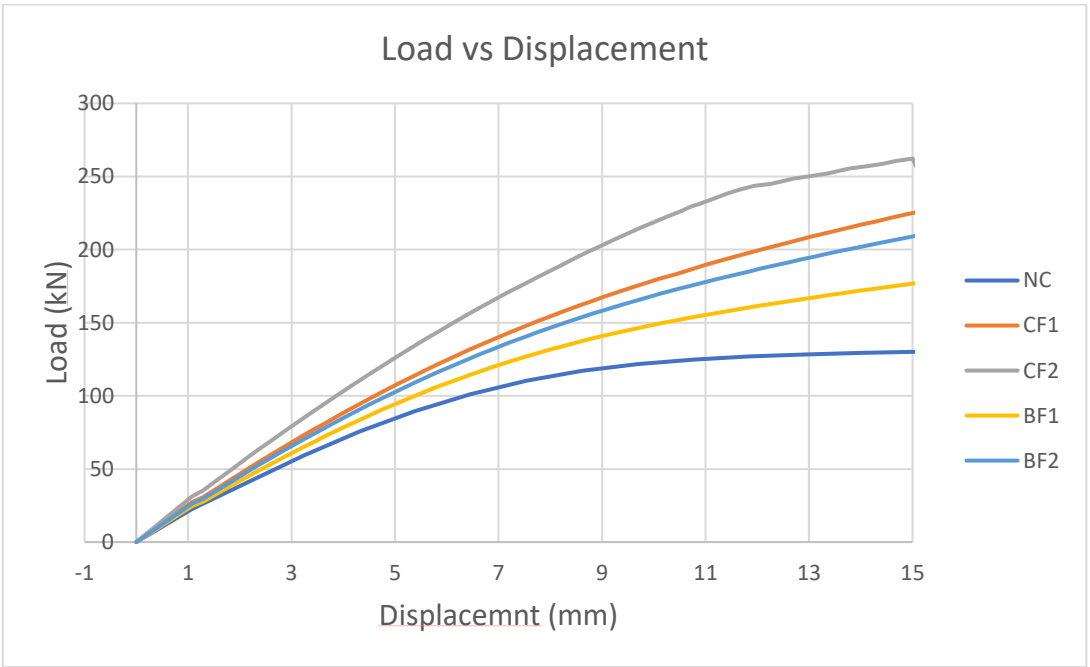

Figure 6.5 Load-displacement curve for CFRP and BFRP retrofitted normal joint

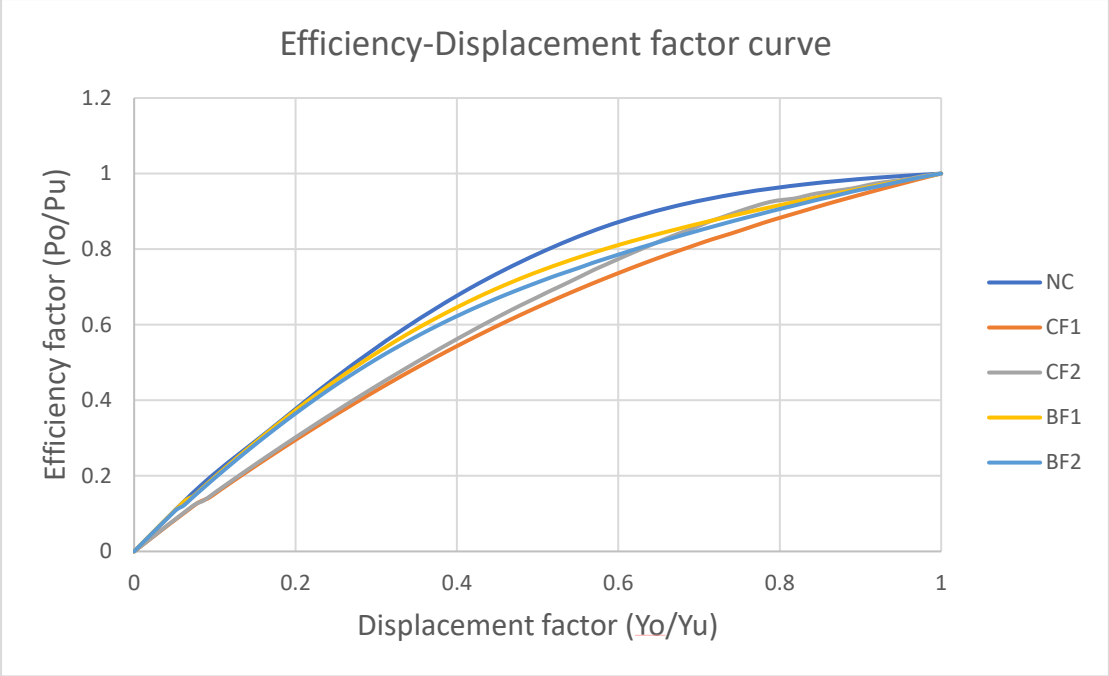

Figure 6.6 Efficiency-displacement factor curve for CFRP and BFRP retrofitted normal joint

6.4 Effect of CFRP and BFRP on Normal Beam Column Joint with Transverse Beam Opening

For analysing the effect of opening in beam column joint two shape of opening square (150 x150mm) and rectangular (300 x150mm) was selected. Also, two distances of opening from joint 150mm and 300mm was adopted.

6.4.1 Effect of CFRP and BFRP on Normal Beam Column Joint with Square Opening

To investigate the effect beam column joint with square opening at a distance of 150mm and 300mm was retrofitted with 1mm and 2mm thickness of CFRP and BFRP fabric. the models are analyzed and the results were compared to the load carrying capacity of a normal joint. Deformed model of retrofitted joint with different FRP is shown in figure 6.7 and figure 6.8 represents the load displacement curve for beam column joint retrofitted with 1 and 2 layers of CFRP and BFRP and that of a normal joint with square opening. According to the graph, Use of FRP fabric increases the load carrying capacity of the joint more than normal beam column joint. The load carrying capacity of a CFRP retrofitted beam column joints was greater than that of BFRP. The load carrying capacity increased with thickness of fabric. The

improvement in the load carrying capacity of retrofitted beam column joint with square transverse beam opening at distance of 150mm from joint models CF1S150, CF2S150, BF1S150 and BF2S150 were 87%,136.6%,44% and 114% higher than NS150. Similarly for models of beam column joint with square transverse beam opening at distance of 300mm CF1S300, CF2S300, BF1S300 and BF2S300 were 123%,175% ,87% and 114% higher than NS300. As shown in figure 6.9, the variation of the efficiency factor and load factor curve for the retrofitted joint is similar in all three cases, indicating that the result is correct.

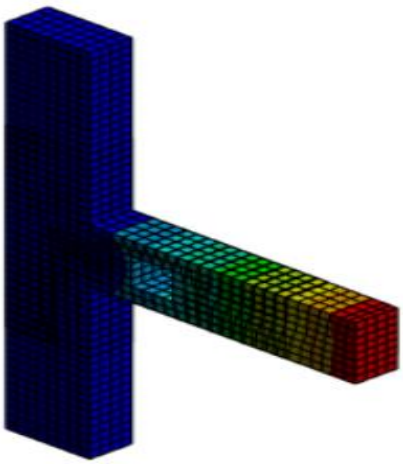

(a) CF1S150

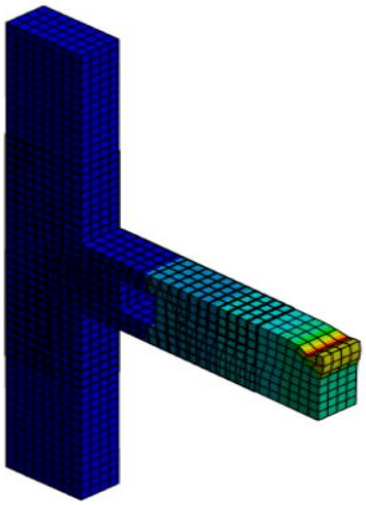

(b) CF2S150

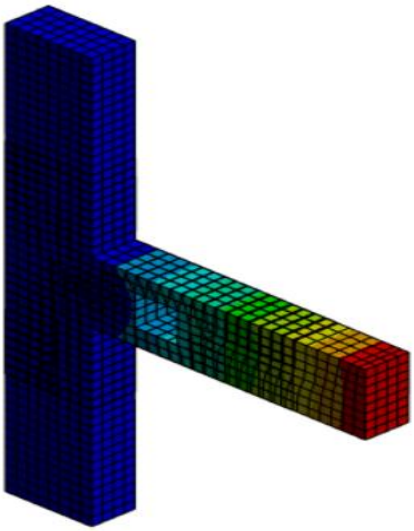

(c) BF1S150

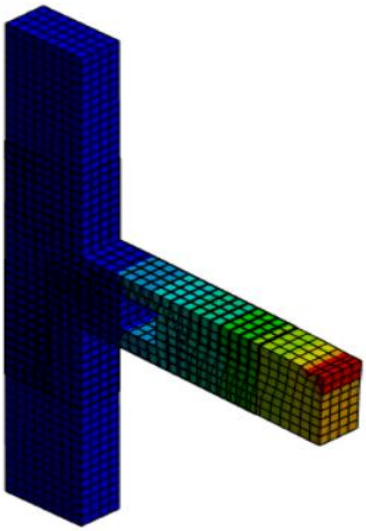

(d) BF2S150

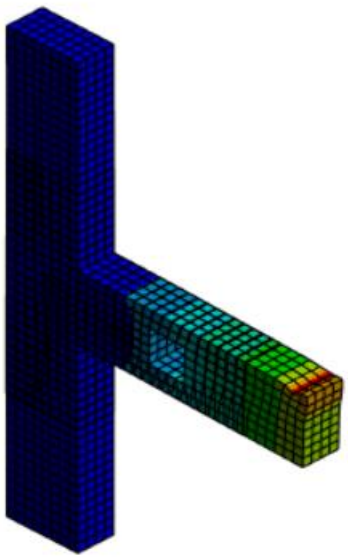

(e) CF1S300

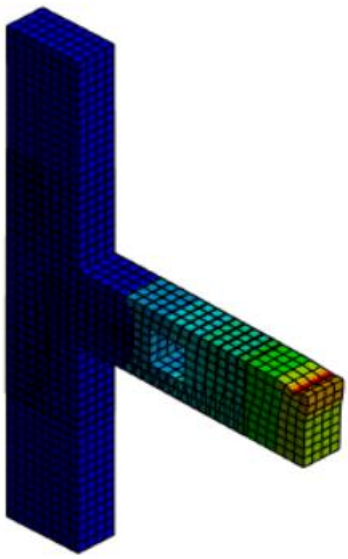

(f) CF2S300

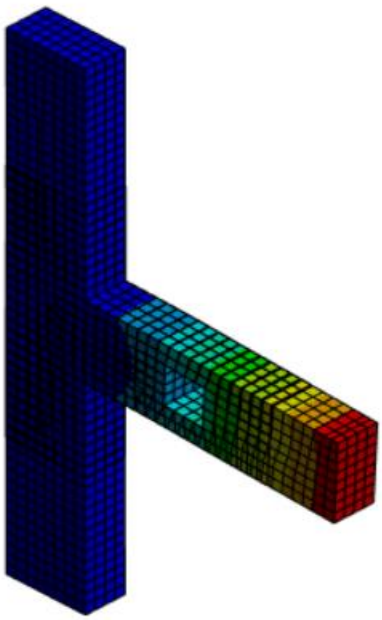

(g) BF1S300

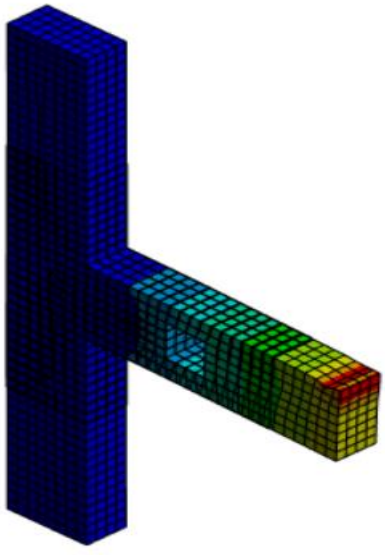

(h) BF2S300

Figure 6.7 Deformed model of retrofitted joint with square opening :(a) CF1S150 (b) CF2S150 (c) BF1S150 (d) BCF1S300 (e) CF1S300 (g) CF2S300 (g) BF1S300 and (h) BF1S300

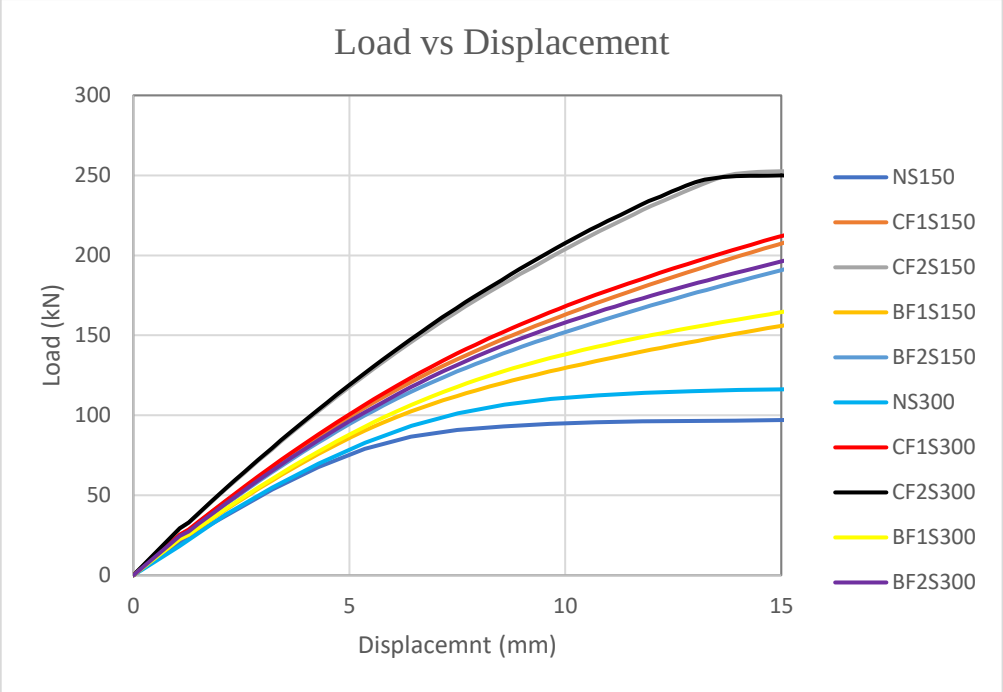

Figure 6.8 Load-displacement curve of Retrofitted BCJ with square opening

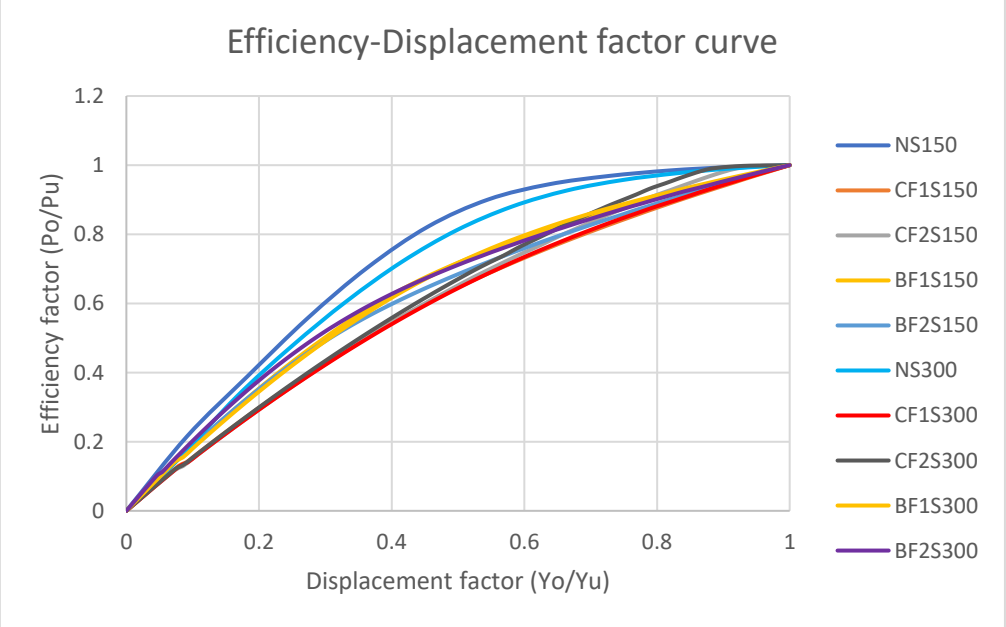

Figure 6.9 Efficiency-displacement factor curve of retrofitted joint with square opening

6.4.2 Effect of CFRP and BFRP on Normal Beam Column Joint with rectangular Opening

To investigate the effect beam column joint with rectangular opening at a distance of 150mm and 300mm was retrofitted with 1mm and 2mm thickness of CFRP and BFRP fabric. the models are analyzed and the results were compared to the load

carrying capacity of a normal joint. Deformed model of retrofitted joint with different FRP is shown in figure 6.10 and figure 6.11represents the load displacement curve for beam column joint retrofitted with 1 and 2 layers of CFRP and BFRP and that of a normal joint with rectangular opening. According to the graph, Use of FRP fabric increases the load carrying capacity of the joint more than normal beam column joint. The load carrying capacity of a CFRP retrofitted beam column joints was greater than that of BFRP. The load carrying capacity increased with thickness of fabric. The improvement in the load carrying capacity of retrofitted beam column joint with rectangular transverse beam opening at distance of 150mm from joint models CF1R150, CF2R150, BF1R150 and BF2R150 were 137%, 227%, 81.5% and 161% higher than NR150. Similarly for models of beam column joint with square transverse beam opening at distance of 300mm CF1R300, CF2R300, BF1R300 and BF2R300 were 123%, 209%, 88% and 176% higher than NR300. As shown in figure 6.12, the variation of the efficiency factor and load factor curve for the retrofitted joint is similar in all three cases, indicating that the result is correct.

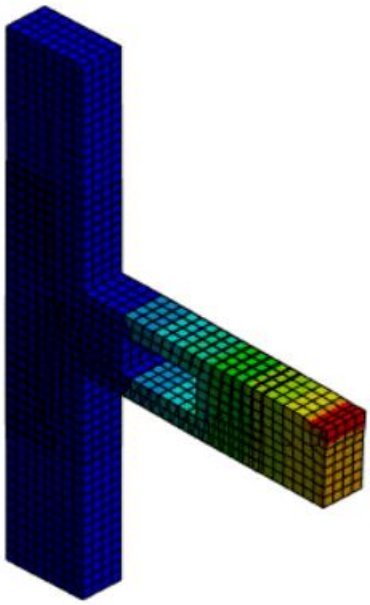

(a) CF1R150

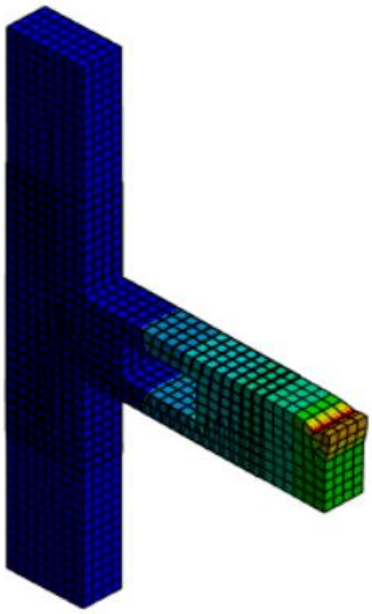

(b) CF2R150

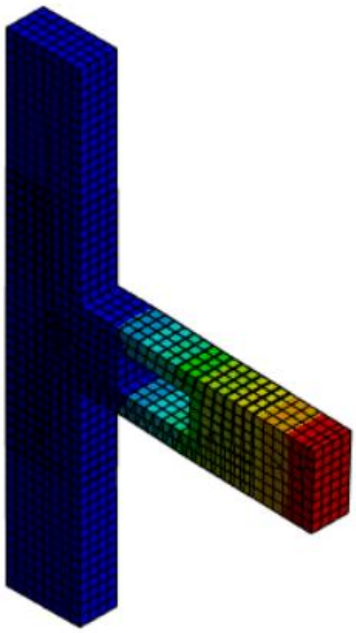

(c) BF1R150

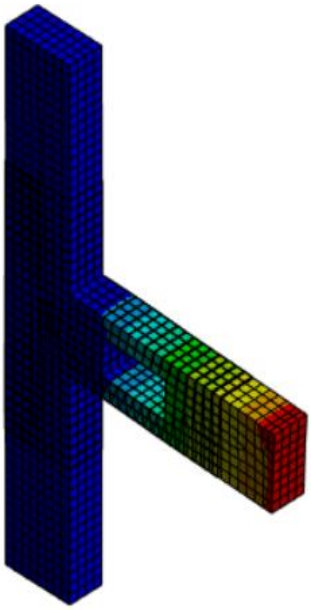

(d) BF2R150

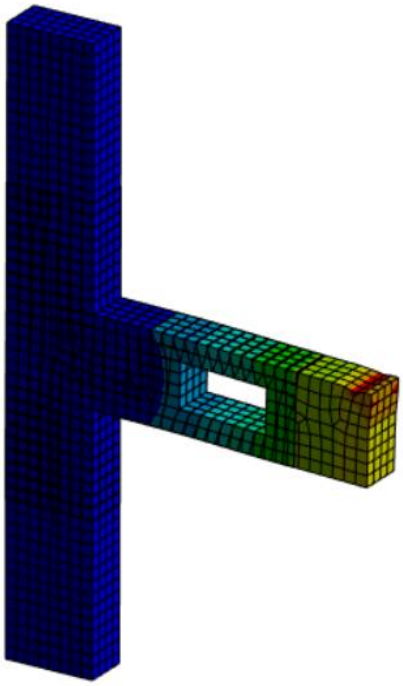

(e) CF1R300

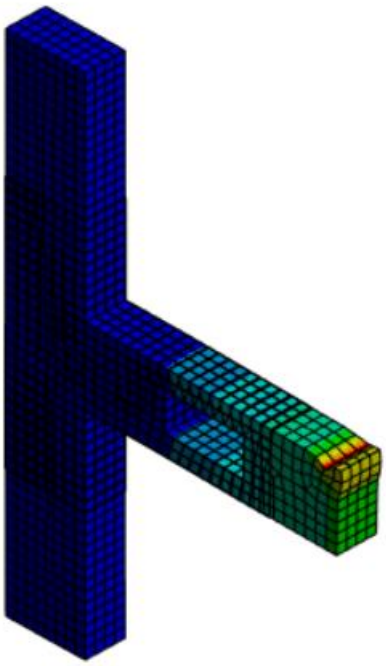

(f) CF2R300

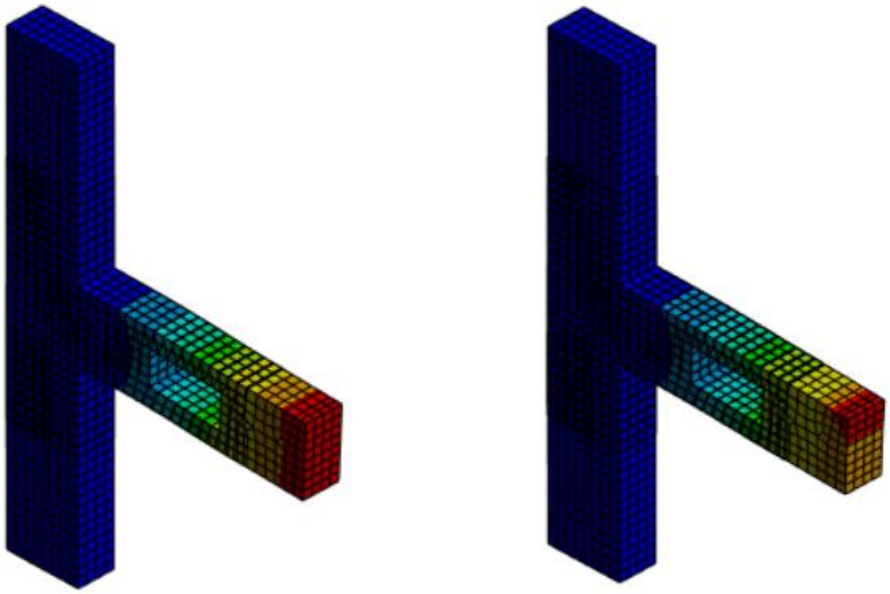

(g) BF1S300 (h) BF2S300

Figure 6.10 Deformed model of retrofitted joint with rectangular opening :(a) CF1R150 (b) CF2R150 (c) BF1R150 (d) BCF1R300 (e) CF1R300 (g) CF2R300 (g) BF1R300 and (h) BF1R300

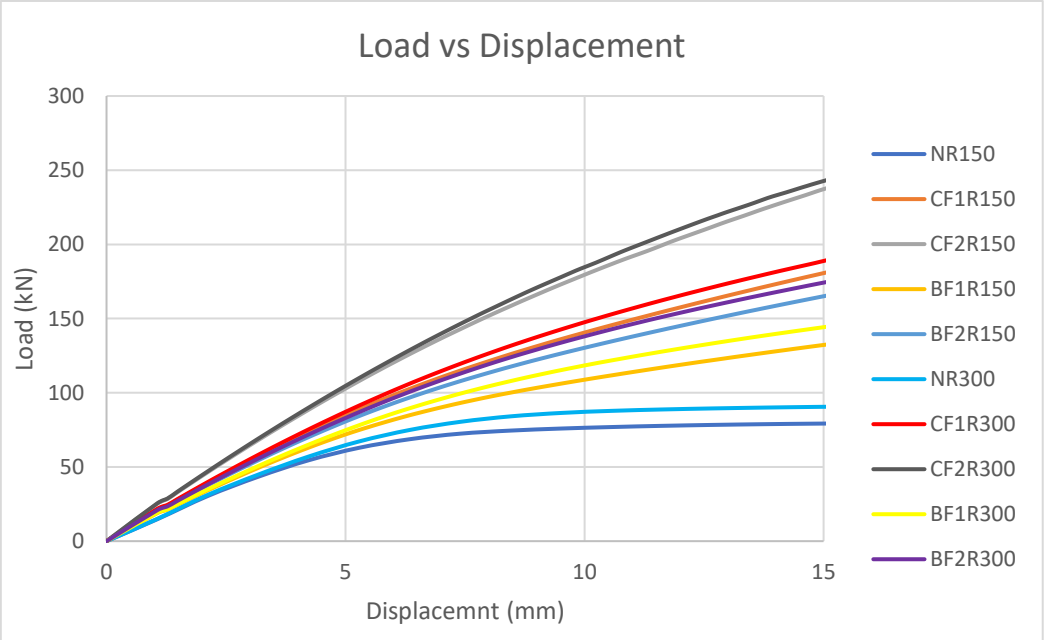

Figure 6.11 Load-displacement curve of Retrofitted BCJ with rectangular opening

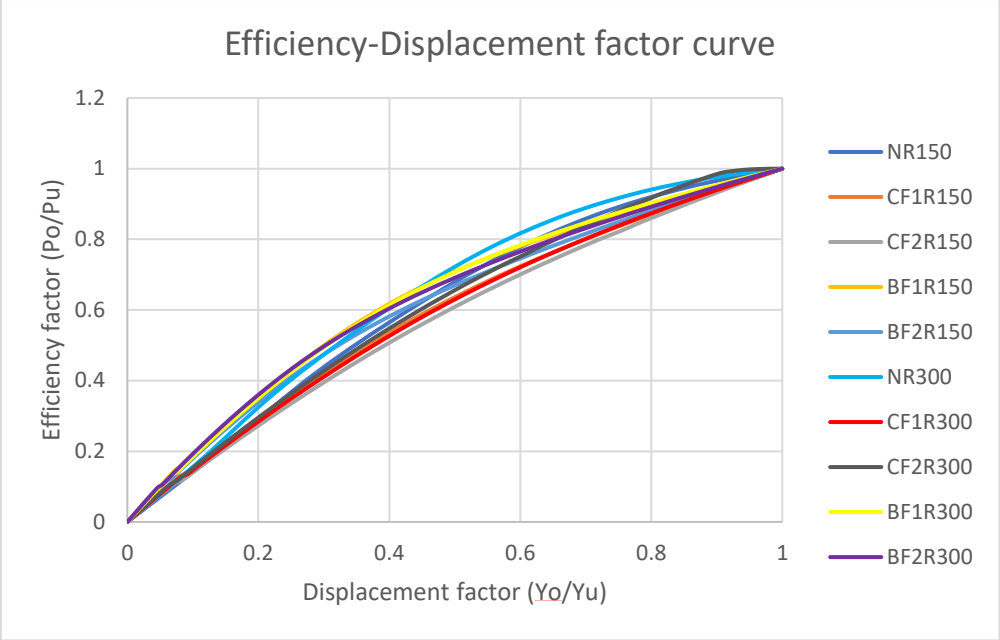

Figure 6.12 Efficiency-displacement factor curve of retrofitted joint with rectangular opening

6.5 First Crack Load

The first crack load of a beam column joint is the load at which the crack begins to form. ANSYS calculates the first crack load by comparing the deformed model and the load versus time curve. Figure 6.13 depicts the deformed model retrofitted with FRP. Table 6.1 compares the first crack load of each model. The first crack load of a normal beam column joint is 101.8 whereas the first crack load has increased to 138.34 and 170.75 for CFRP retrofitted and 117.13 and 131.88 for BFRP retrofitted. Similar increase can be seen in all retrofitted models of beam column joints with transverse beam opening shown in Table 6.1. The CFRP fabric retrofitted models have a greater first crack load than other models. Increase in thickness of FRP retrofitting increased the first crack load for both CFRP and BFRP. The strong link produced between the injected epoxy and the concrete prevented fracture propagation within the concrete as well as crack propagation within the initially undamaged concrete of the enhanced specimen.

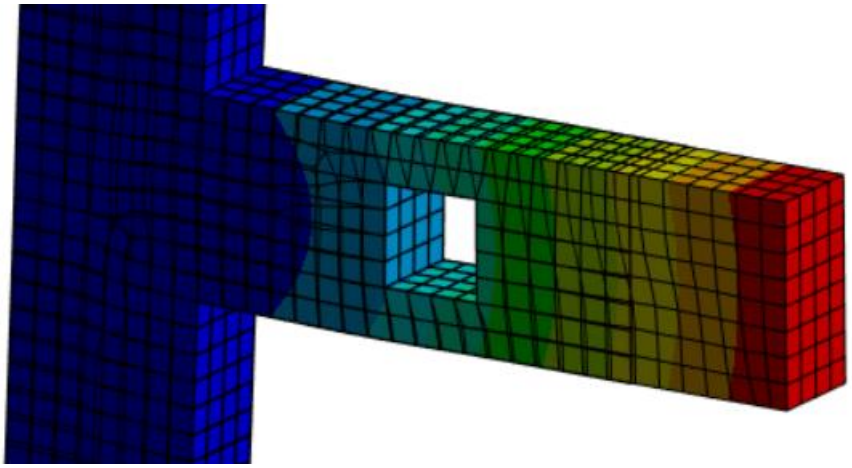

Figure 6.13 Crack formation in retrofitted model

Table 6.1 First crack load of beam column joint models

Specimen	First crack load (kN)
NC	101.08
CF1	138.34
CF2	170.75
BF1	117.13
BF2	131.88
BCJ with square opening at a spacing of 150mm from joint	
NS150	67.717
CF1S150	99.483
CF2S150	124.59
BF1S150	81.928
BF2S150	94973
BCJ with square opening at a spacing of 300mm from joint	
NS300	82.893
CF1S300	113.46
CF2S300	141.08

BF1S300	95.783
BF2S300	108.34
BCJ with rectangular opening at a spacing of 150mm from joint	
NR150	43.415
CF1R150	84.634
CF2R150	108.01
BF1R150	63.118
BF2R150	73.213
BCJ with rectangular opening at a spacing of 300mm from joint	
NR300	57.082
CF1R300	94.586
CF2R300	117.66
BF1R300	74.514
BF2R300	87.126

6.6 Comparison of Models in Terms of Ductility, Energy Dissipation Capacity and Stiffness Degradation

6.6.1 Cyclic Loading

Understanding of load-displacement hysteretic response is crucial for assessing their seismic performance of any analysis. It allows for the assessment of ductility and energy dissipation, two critical aspects of structural performance under lateral stresses. Which can be used to assess the cyclic performance of beam-column joint. Figure 6.14 depicts the cyclic loading history applied to the models. Push values are shown by positive hysteretic plots, whereas pull values are represented by negative region curves.

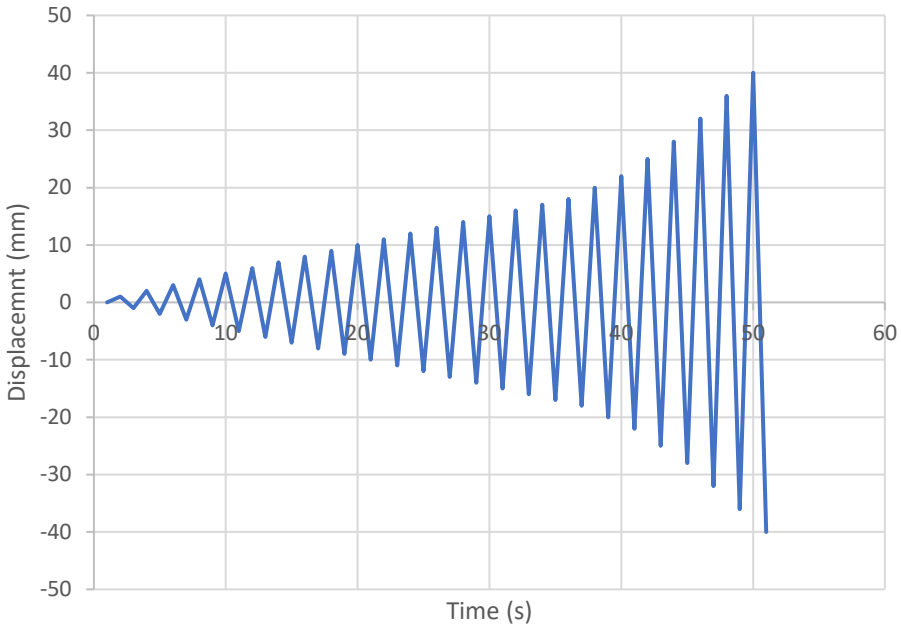

Figure 6.14 Cyclic loading history

The hysteretic behaviour of the external joint was evaluated in terms of ductility, energy dissipation capacity, and stiffness degradation. Figures 6.15 show that the ultimate loads and deformation capabilities for models with transverse beam opening. Due to opening the area of loop decreases. The hysteretic response of CFRP and BFRP retrofitted normal joint is shown in figure 6.16. The increase sharpness of loop is primarily because externally bonded CFRP and BFRP fabric. The hysteresis loop in Figures 6.17 and 6.18 represents the hysteretic behaviour of FRP retrofitted models with transverse beam of square and rectangular opening. The increase in ultimate load is more for CFRP fabric retrofitted models than BFRP retrofitted. During the elastic stage, the loop's area remained steady under both push and pull stresses. The cracking stage then started, causing stiffness loss in the specimen as the area of the loop increased with each loading cycle.

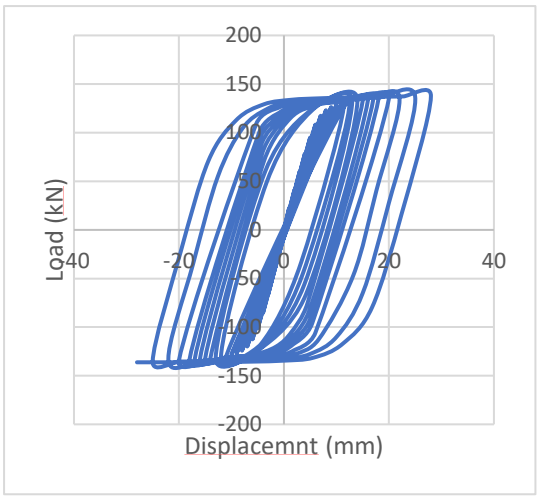

(a) NC

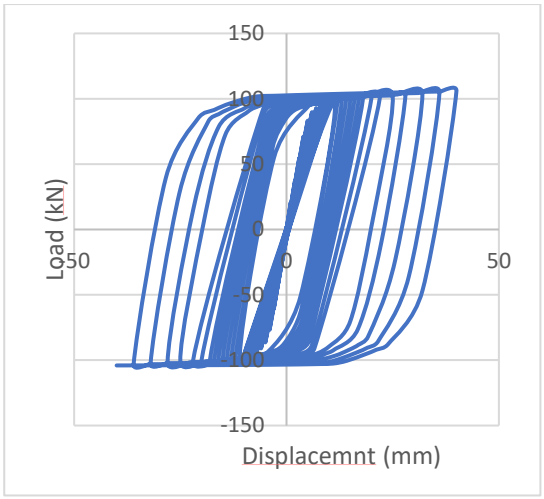

(b) NS150

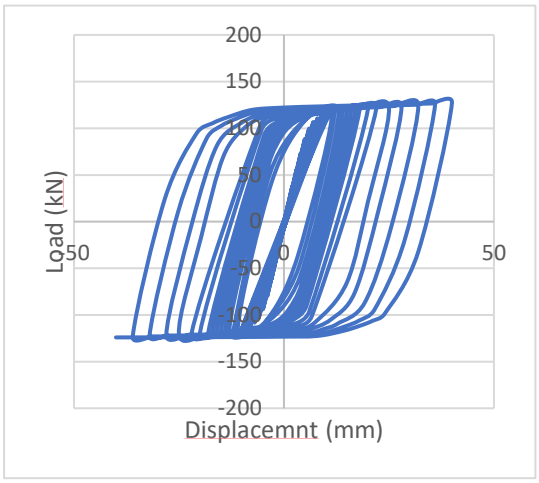

(c) NS300

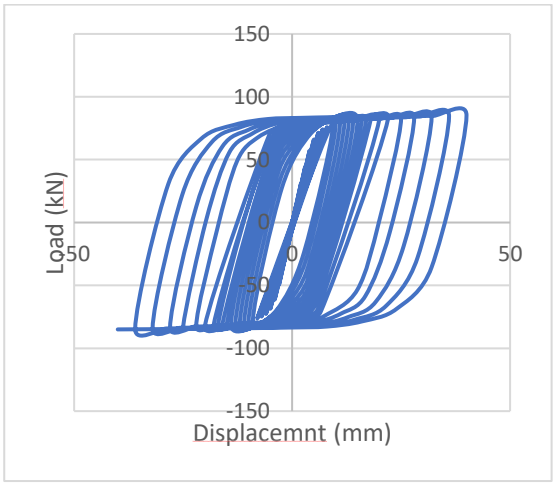

(d) NR150

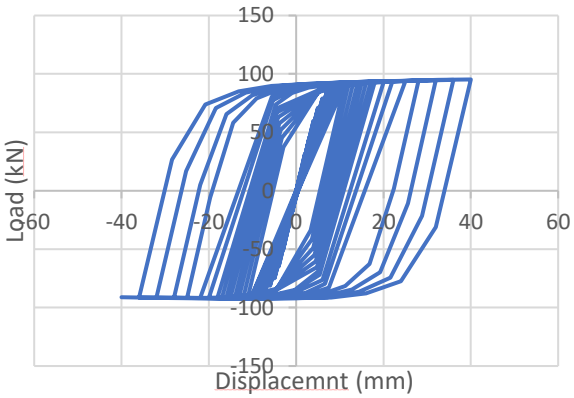

(e) NR300

Figure 6.15 Hysteretic response of joint with opening: (a) NC (b) NS150 (c) NS300 (D) NR150 and (E) NR300

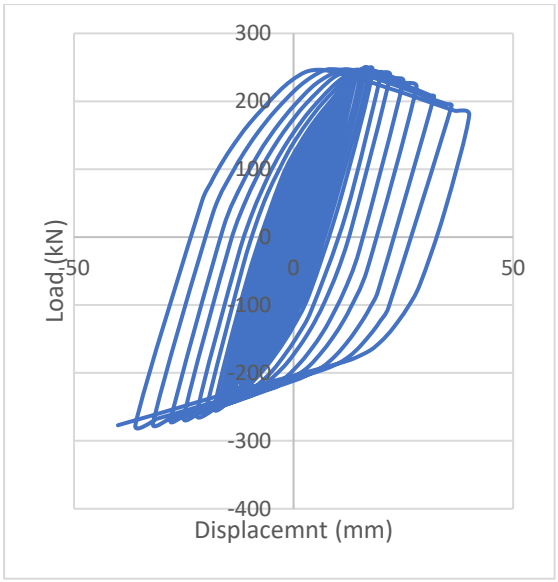

(a) CF1

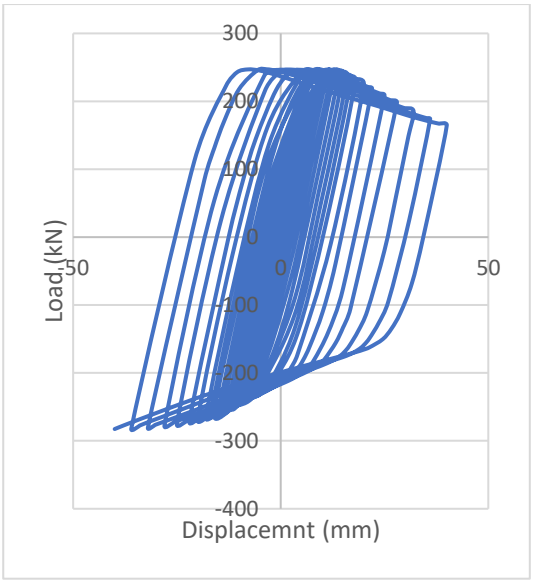

(b) CF2

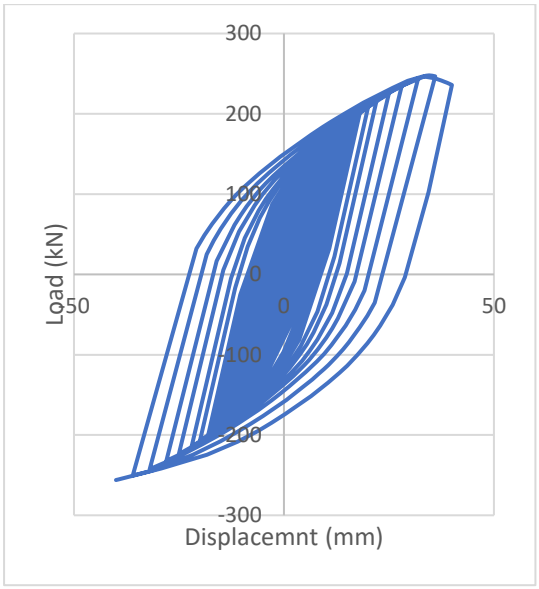

(c) BF1

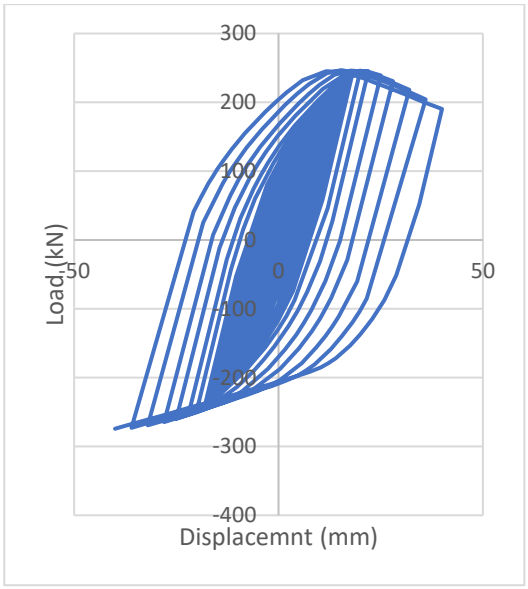

(d) BF2

Figure 6.16 Hysteretic response of retrofitted normal joint:(a) CF1 (b) CF2 (c) BF1 and (d) BF2

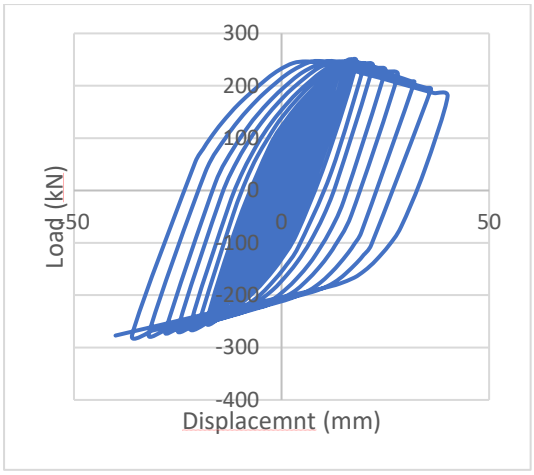

(a) CF1S150

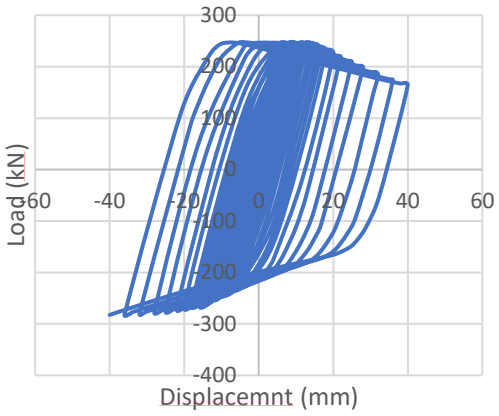

(b) CF2S150

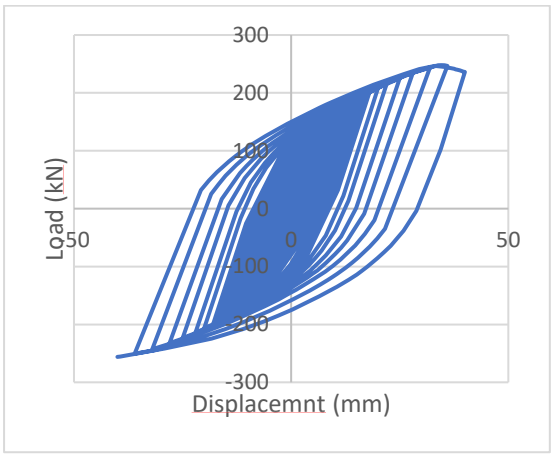

(c) BF1S150

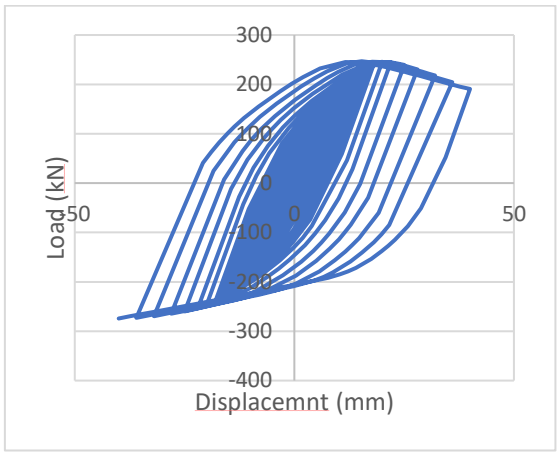

(d) BF2S150

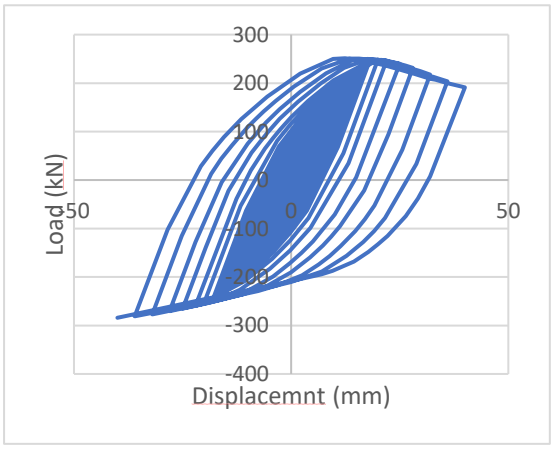

(e) CF1S300

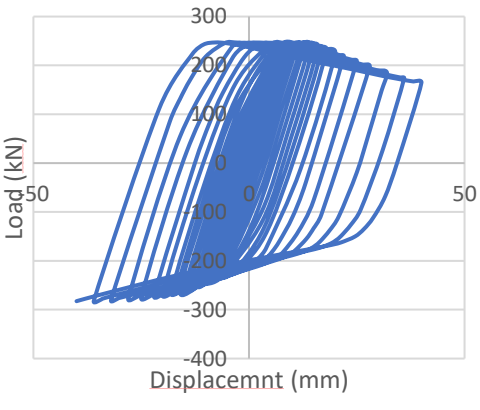

(f) CF2S300

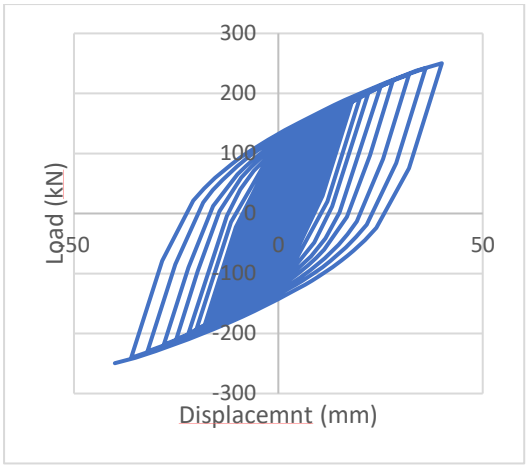

(g) BF1S300

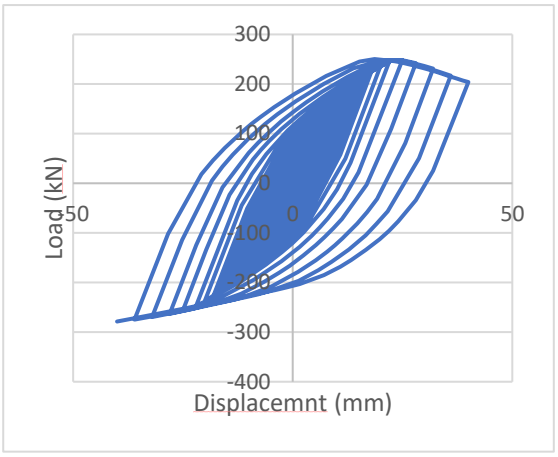

(h) BF2S300

Figure 6.17 Hysteretic response of retrofitted joint of retrofitted joint with square opening :(a) CF1S150 (b) CF2S150 (c) BF1S150 (d) BCF1S300 (e) CF1S300 (g) CF2S300 (g) BF1S300 and (h) BF1S300

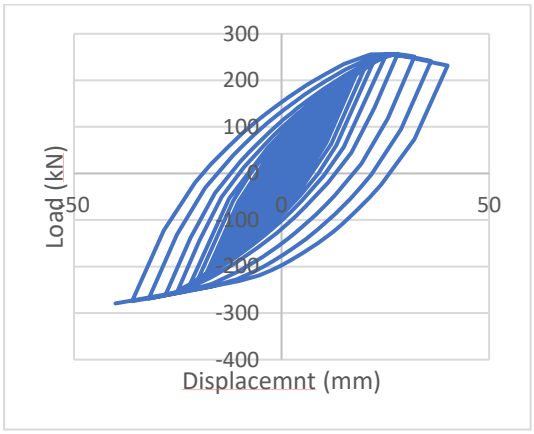

(a) CF1S150

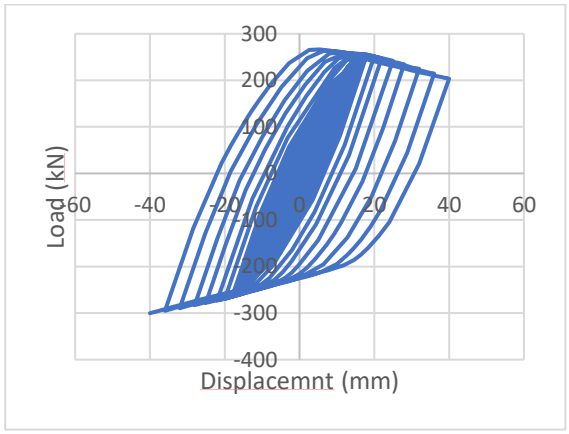

(b) CF2S150

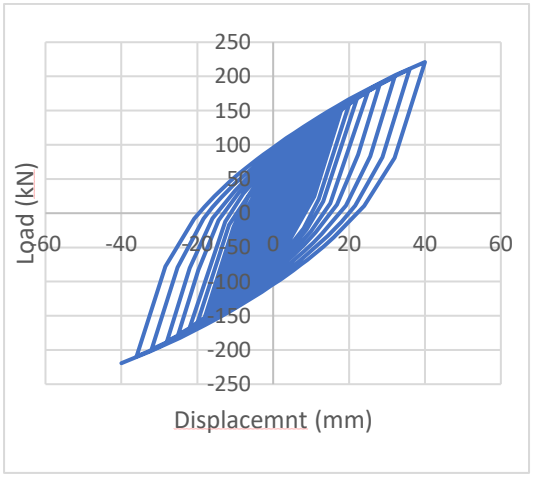

(c) BF1S150

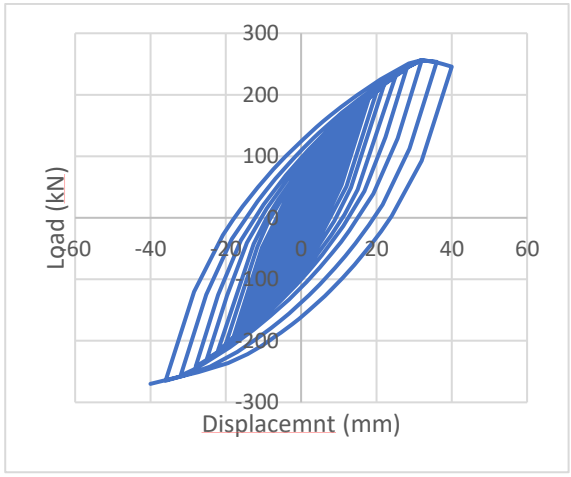

(d) BF2S150

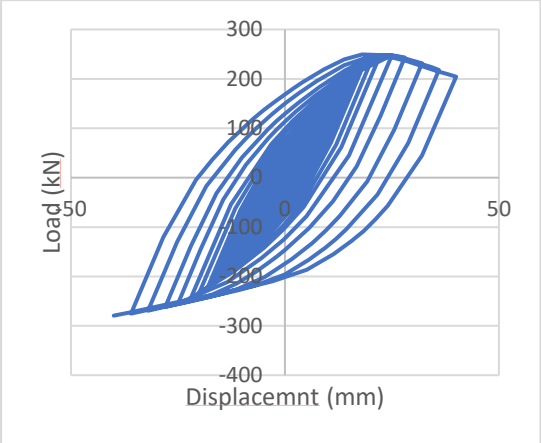

(e) CF1S300

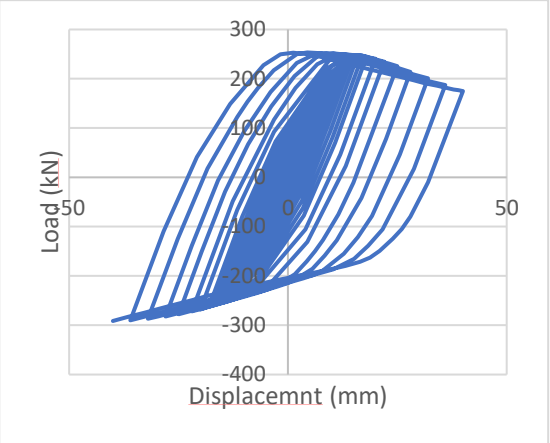

(f) CF2S300

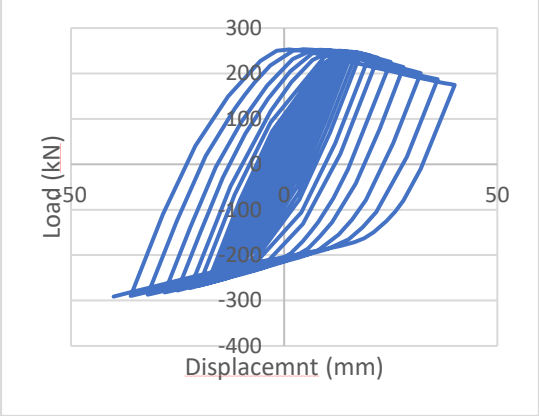

(g) BF1S300

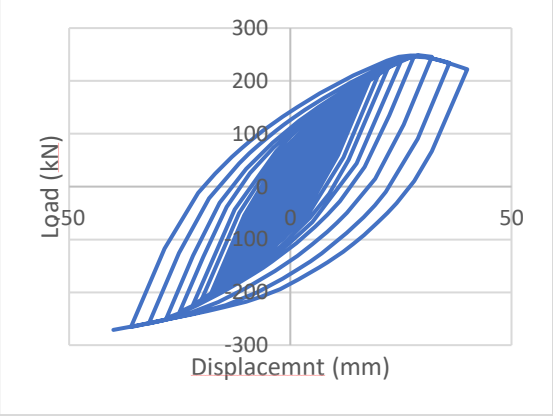

(h) BF2S300

Figure 6.18 Hysteretic response of retrofitted joint with rectangular opening: (a) CF1R150 (b) CF2R150 (c) BF1R150 (d) BCF1R300 (e) CF1R300 (g) CF2R300 (g) BF1R300 and (h) BF1R300

6.6.2 Ductility

Ductility of a structure and its elements is defined as its ability to tolerate large inelastic deformation without appreciably losing strength is characterised as ductility During inelastic cyclic deformations, ductile structures can dissipate hysterically large amounts of energy. The term ductility is an important characteristic measure for quantifying a structure's or element's seismic behaviour. The performance of the retrofitted models is compared in this section in terms of ductility. A ductile structure can dissipate

significant amounts of energy in a hysteretic mode during inelastic cyclic motions. A ductile structure can dissipate significant amounts of energy in a hysteretic mode during inelastic cyclic motions. The displacement ductility is defined as the maximum displacement divided by the yield displacement The method used to determine curvature ductility, commonly known as the ductility factor, is based on that given by Lee and Pan (2003). Hence, the ductility factor (μ_ϕ) can be given by:

$$\mu = d_u / d_y$$

In which: ϕ_u is the ultimate curvature of the analysed cross section; ϕ_y is the yielding curvature at the same cross section.

Table 6.2 shows the maximum and yield displacement values, as well as the ductility of the numerically analysed models. It can be seen that all joints had good seismic performance. The usage of CFRP and BFRP increases ductility as compared to normal joints. Because BFRP is more ductile than CFRP, the ductility of BFRP retrofitted models are higher. Increase in number of layers of FRP boosted the ductile capacity of the junction substantially. The ductility increase is more for FRP retrofitted beam column joint with square opening than for rectangular opening. Ductility is determined by the type of FRP. Table 6.2 compares the ductility ratio of each model, FRP is very much effective in ductility improvement condition. It increases the ductility by 3%, 4.5% and 32.5%, 87% in case of CFRP and BFRP strengthened one and two layers when compared to normal beam column joint (NC). When in case of retrofitted models with different combination of size and location of opening all the models differ in ductility greatly compared to normal joints. In case of strengthened beam column joint with square opening at a distance of 150mm from joint the increase in ductility for 1, 2 layers CFRP and BFRP are 40%, 40.5% and 55.5%, 111% when compared to NS150 and 71.4%, 75.7% and 109.3% and 293% compared to NS300 in case of square opening at a distance of 300mm. The increase in ductility in case of rectangular opening at a distance of 150mm is 18.4%, 21.8% and 50.2%, 84.5% when compared to NR150 and 42.6%, 69.7% and 91.4% and 157.7% compared to NR300 in case of rectangular opening at a distance of 300mm

Table 6.2 Displacement ductility factor for models

Specimen	Displacement at yield (mm)	Displacement at maximum load (mm)	Ductility factor	% Variation
NC	6.4587	12.916	2	-
CF1	6.878	14.07	2.06	3
CF2	7.179	15	2.09	4.5
BF1	6.6736	17.651	2.65	32.5
BF2	6.8821	25.764	3.74	87
BCJ with square opening at a spacing of 150mm from joint				
NS150	4.287	8.5901	2	-
CF1S150	5.0292	14.085	2.8	40
CF2S150	5.3402	14.982	2.81	40.5
BF1S150	4.7133	14.674	3.11	55.5
BF2S150	5.0314	21.264	4.22	111
BCJ with square opening at a spacing of 300mm from joint				
NS300	5.3639	7.4965	1.4	-
CF1S300	5.7814	13.877	2.4	71.4
CF2S300	6.0891	15.023	2.46	75.7
BF1S300	5.5749	16.332	2.93	109.3
BF2S300	5.7845	23.785	4.11	293
BCJ with rectangular opening at a spacing of 150mm from joint				
NR150	3.173	7.3909	2.33	-
CF1R150	4.9746	13.757	2.76	18.4
CF2R150	5.288	15.019	2.84	21.8
BF1R150	4.2338	14.821	3.5	50.2

BF2R150	4.4463	19.061	4.3	84.5
BCJ with rectangular opening at a spacing of 300mm from joint				
NR300	4.2329	7.4054	1.75	-
CF1R300	5.5063	13.775	2.5	42.8
CF2R300	5.7108	16.975	2.97	69.7
BF1R300	4.9783	16.678	3.35	91.4
BF2R300	5.2961	23.886	4.51	157.7

6.6.3 Energy dissipation capacity

Energy dissipation is another parameter which is used to assess the seismic performance. In RC structures, energy dissipation includes energy dissipated by steel reinforcements, energy dissipated during crack growth, and friction between crack surfaces. Certain structural members are capable of withstanding massive deformations. As a result, they diffuse energy and mitigate the impacts of seismic pressures on the structure. When a building is subjected to a violent earthquake, a building with a better energy dissipation capability can absorb more energy, eventually ending in the building collapsing. Inelastic action causes energy dissipation. The energy dissipated in each cycle is defined as the area under the cycle in a specimen's cyclic response. The energy loss due to inelastic action in that cycle is equal to the area contained within a hysteretic loop. The higher the dissipation of energy, the fatter the cycle. Cumulative energy dissipation is the sum of the energy dissipated in successive loops throughout the test.

Figures 6.19 depict the cumulative energy dissipation versus drift ratio for normal joints with opening. Total energy capacity increases with opening size and also increases with distance of opening from joint. Figures 6.20–6.22 depict the cumulative energy dissipation versus drift ratio for retrofitted models of normal joints, retrofitted joint with square opening and retrofitted joint with rectangular opening. Table 6.3 displays the total energy dissipation capacity of all beam column joint models. All of the retrofitted models outperformed the standard beam column joint in terms of energy dissipation,

demonstrating that the rehabilitation strategy is effective. Total energy dissipation is more for CFRP strengthened models. The energy absorption is same for all models up to 1% drift ratio. After a 1% drift ratio, energy dissipation began to rise significantly for all the models when retrofitted with FRP fabrics, as shown in figure 6.20-6.22. BFRP retrofitted models shows decreased total energy absorption for single layer thickness. As the layer thickness increases the dissipation also increases. It was determined that joints rehabilitated using the proposed strengthening system dissipate more energy than the control when subjected to large lateral displacements of other structural members, ensuring the structure's safety.

Table 6.3 Total energy dissipation capacity of models

Specimen	Total Energy Dissipation Capacity (kNm)
NC	0.387
CF1	5.58
CF2	6.8
BF1	1.48
BF2	4.85
BCJ with square opening at a spacing of 150mm from joint	
NS150	0.907
CF1S150	5.41
CF2S150	7.06
BF1S150	0.32368
BF2S150	3.95
BCJ with square opening at a spacing of 300mm from joint	
NS300	1
CF1S300	5.41
CF2S300	7.19
BF1S300	0.287
BF2S300	4.5
BCJ with rectangular opening at a spacing of 150mm from joint	

NR150	0.6
CF1R150	3.4
CF2R150	5.98
BF1R150	0.345
BF2R150	1.95
BCJ with rectangular opening at a spacing of 300mm from joint	
NR300	0.66
CF1R300	4.14
CF2R300	10.2
BF1R300	1.03
BF2R300	2.38

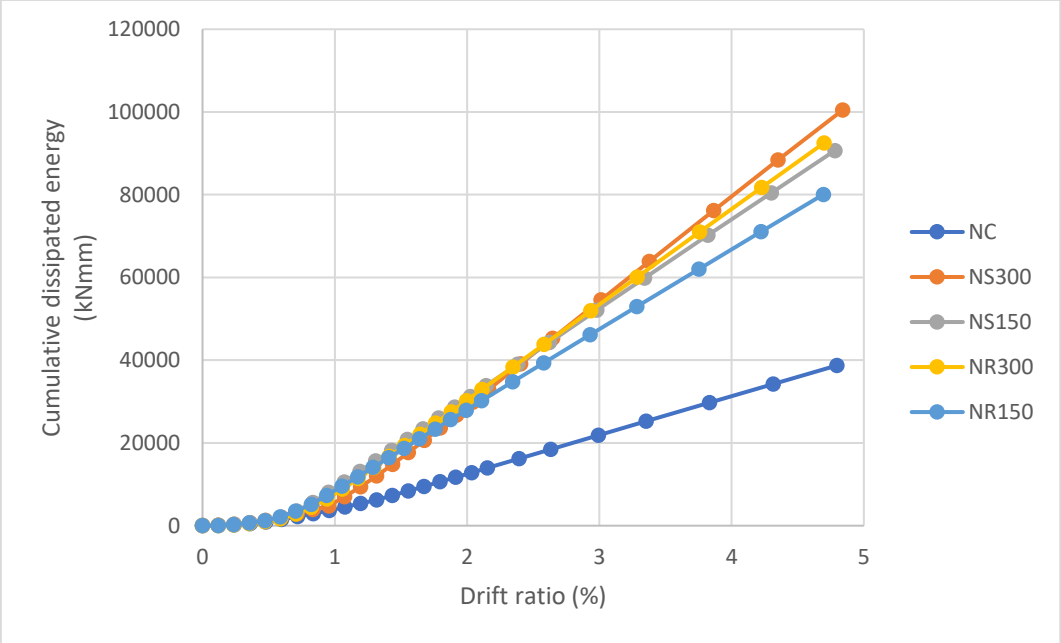

Figure 6.19 Cumulative energy dissipation against drift ratio for normal joint with different opening

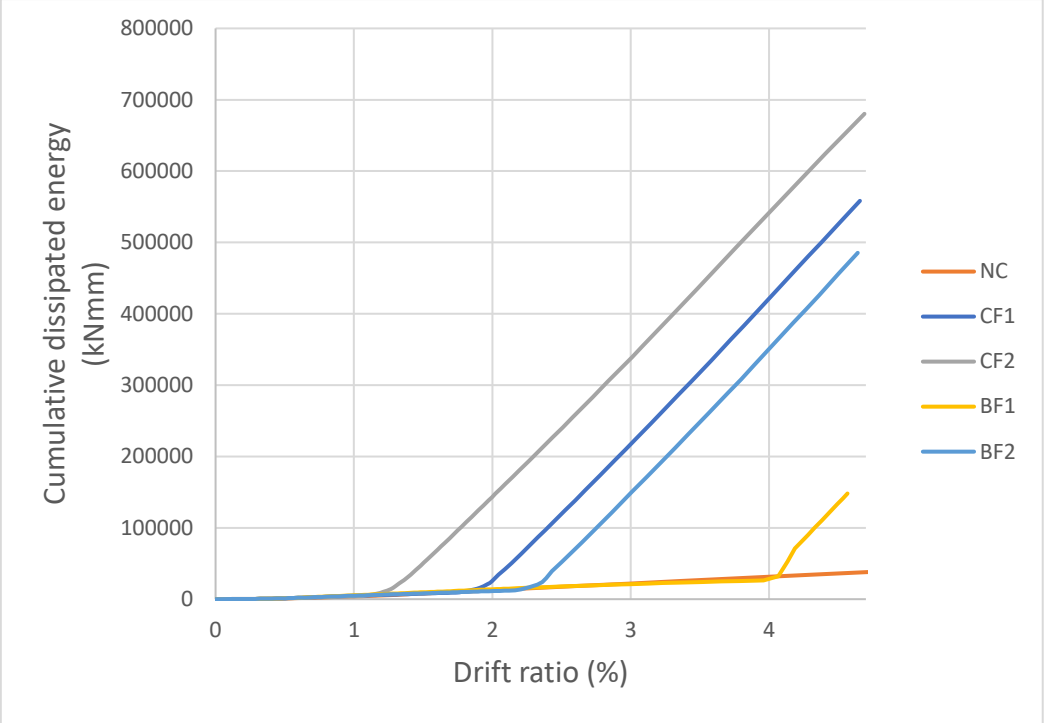

Figure 6.20 Cumulative energy dissipation against drift ratio for retrofitted normal joint

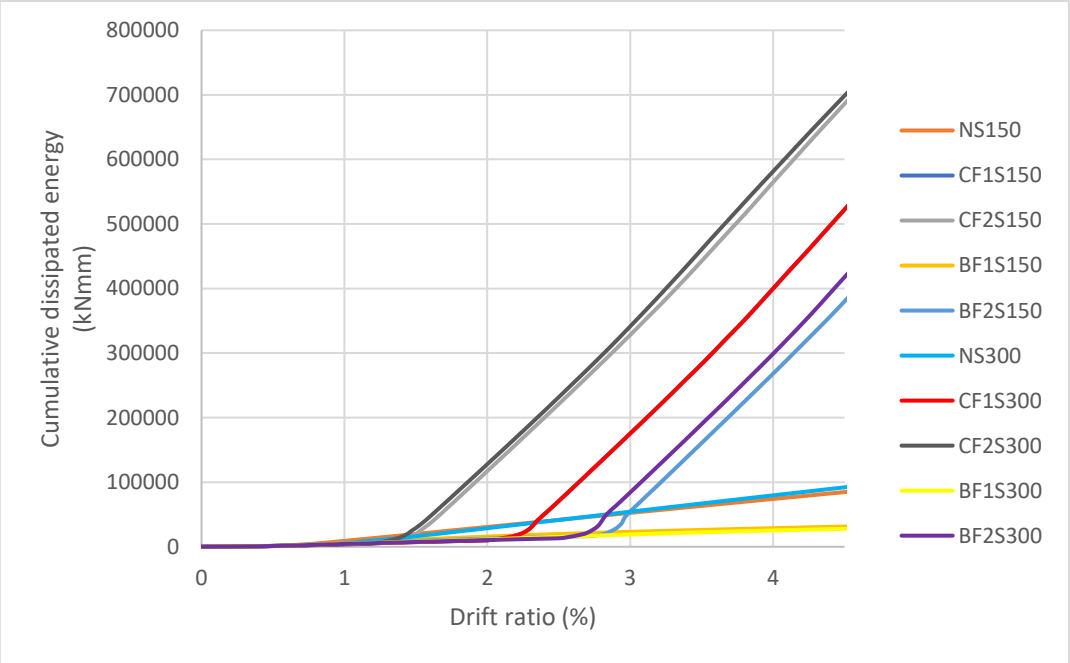

Figure 6.21 Cumulative energy dissipation against drift ratio for retrofitted joint with square opening

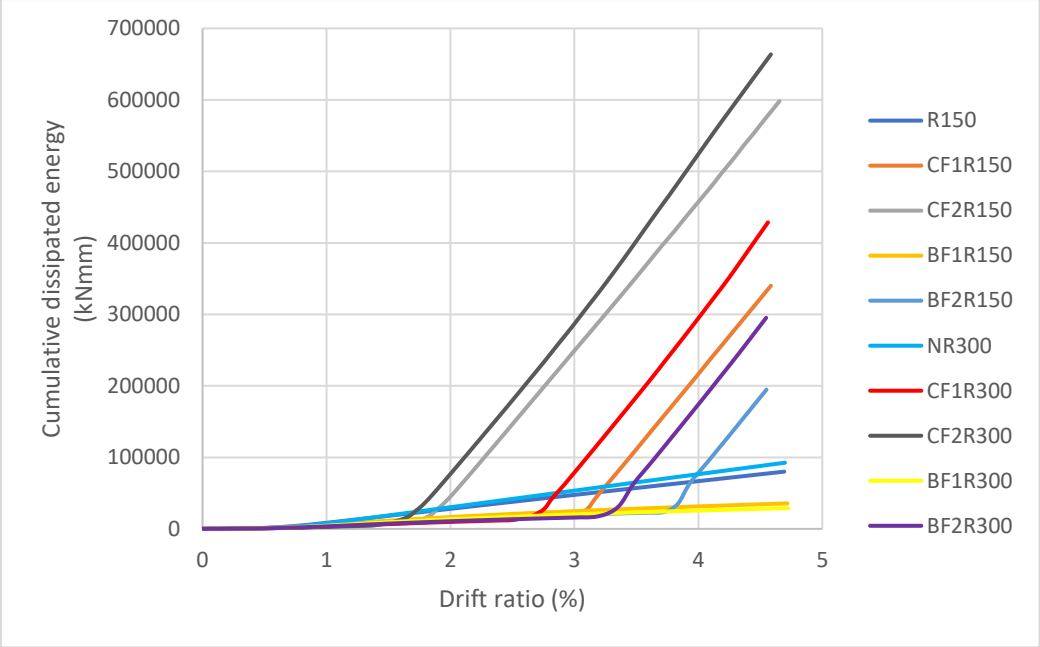

Figure 6.22 Cumulative energy dissipation against drift ratio for retrofitted joint with rectangular opening

6.6.4 Stiffness degradation

Stiffness degradation is the loss of stiffness when the lateral movement of a structure increases. In other words, when the load on the specimen increases, the required force for a given displacement reduces. Flexural and shear cracks, shear deformation of the connection core, loss of cover, concrete nonlinear behaviour, longitudinal rebar yielding, concrete compression failure, longitudinal rebar slippage, longitudinal steel failure or buckling, and second-order forces all erode a concrete structure's stiffness. The low rate of strength degradation is crucial for RC constructions in mild earthquakes, when non-structural materials can sustain some damage but structural elements must be strong enough to remain elastic and avoid destruction. The increased initial stiffness and lower rate of stiffness degradation will improve the behaviour of the beam column joint during an earthquake. In general, as the cycle numbers increase, the stiffness of the beam column joint decreases gradually. As a result, at each drift ratio, the joint cyclic stiffness is defined as the slope of the line connecting the maximum points of the first reversal cycle in the lateral load-displacement response, which can be expressed as follows:

$$K_{i=}(P_i^{+}-P_i^{-})/(d_i^{+}-d_i^{-})$$

where Pi and di are the maximum load and corresponding displacement in either the positive or negative direction. Table 6.4 shows the initial stiffness value for each model. Figures 6.23 show the stiffness degradation versus drift ratio of joint with different opening. In this case, the initial stiffness decreases with the size of opening. Distance of opening from joint has negligible effect. is more than the other materials stiffness, but eventually it degrades and reaches value lesser than single material. Figures 6.24 to 6.26 show the stiffness degradation versus drift ratio of retrofitted normal joint, retrofitted joint with square opening and retrofitted joint with rectangular opening. This is due to the fact that the retrofitted specimen was created by externally bonding FRP sheets to an undamaged concrete specimen. Almost all retrofitted specimens in the case of different combinations shows similar stiffness characteristic. The initial stiffness is more for retrofitted models. CFRP retrofitted models shows higher initial stiffness than BFRP retrofitted models, but stiffness degradation rate is less for BFRP retrofitted models.

Table 6.4 Initial stiffness of models

Specimen	Initial stiffness (kN/mm)
NC	20.95
CF1	23.65
CF2	27.27
BF1	21.26
BF2	29.44
BCJ with square opening at a spacing of 150mm from joint	
NS150	19.23
CF1S150	21.98
CF2S150	25.53

BF1S150	21
BF2S150	21.16
BCJ with square opening at a spacing of 300mm from joint	
NS300	17.71
CF1S300	22.2
CF2S300	25.73
BF1S300	21.25
BF2S300	21.38
BCJ with rectangular opening at a spacing of 150mm from joint	
NR150	14.91
CF1R150	18.91
CF2R150	22.29
BF1R150	17.79
BF2R150	19.4
BCJ with rectangular opening at a spacing of 300mm from joint	
NR300	15.27
CF1R300	19.17
CF2R300	23
BF1R300	18.1
BF2R300	19.7

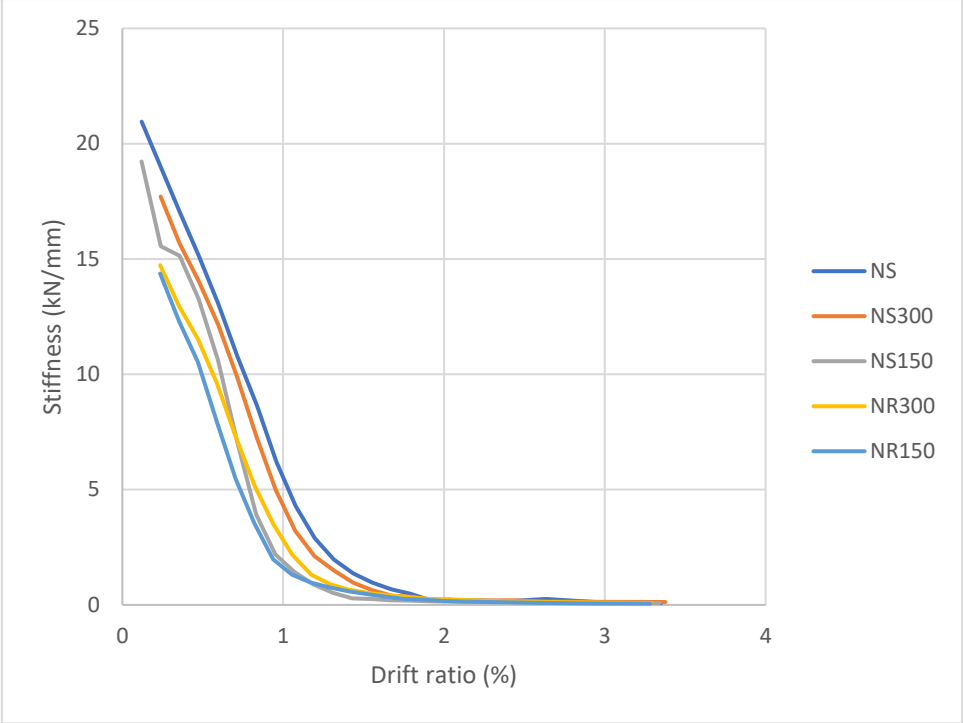

Figure 6.23 Stiffness degradation against drift ratio curve for normal joint with different opening

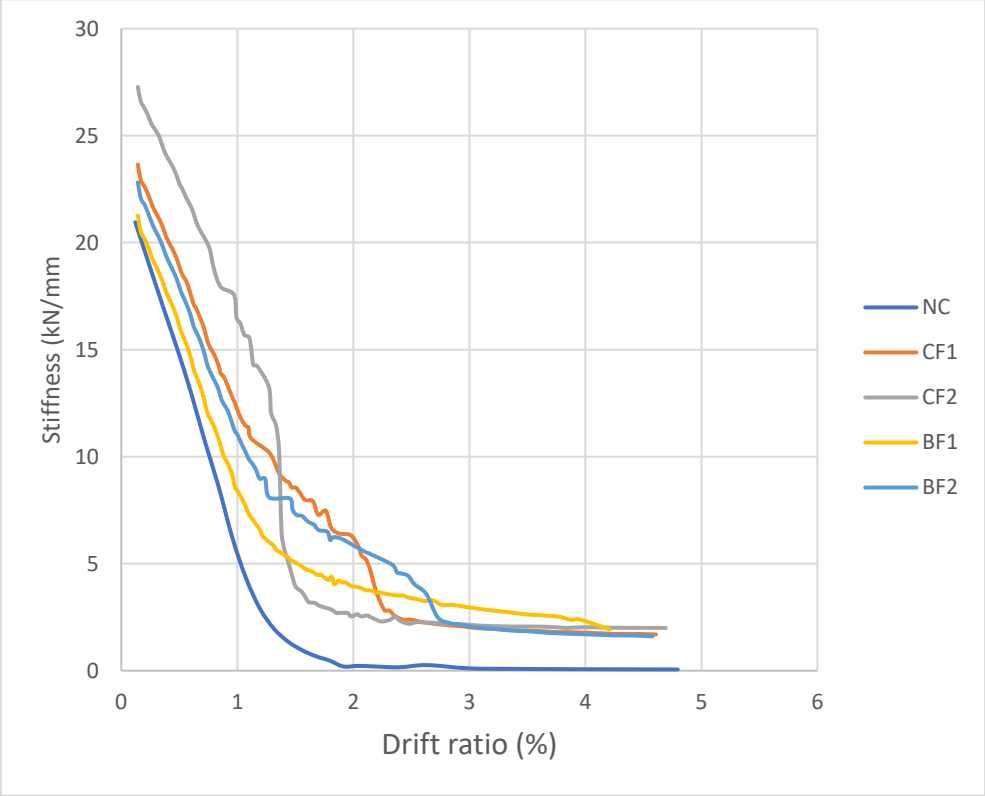

Figure 6.24 Stiffness degradation against drift ratio curve for retrofitted normal joint

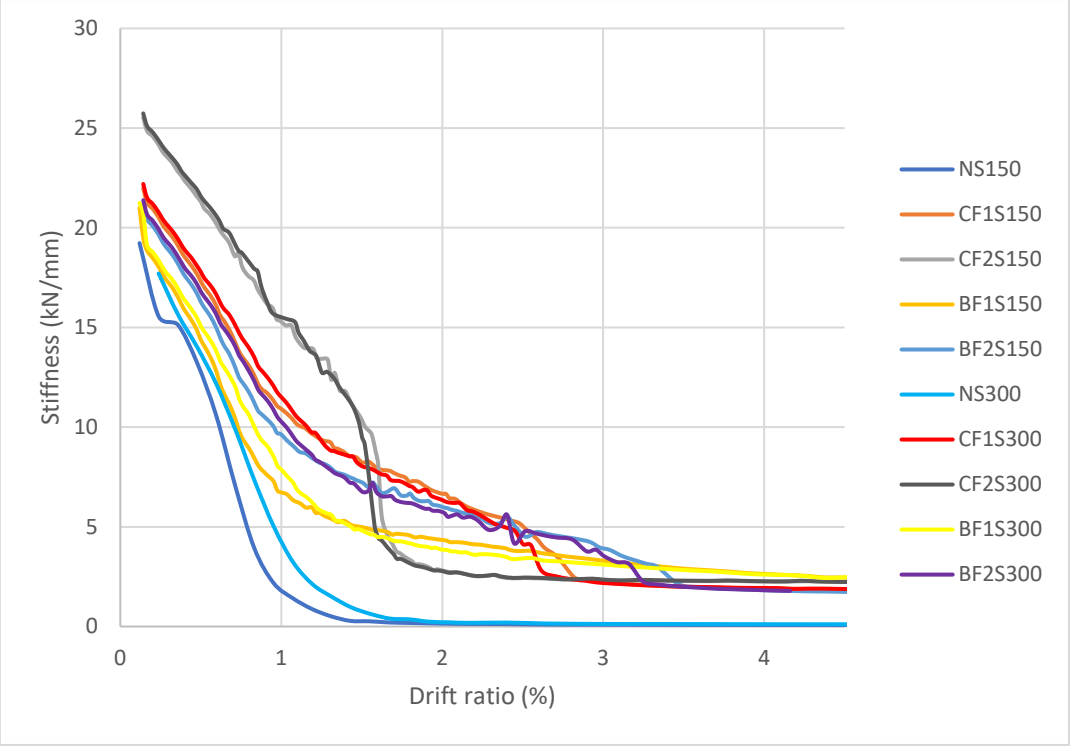

Figure 6.25 Stiffness degradation against drift ratio curve for retrofitted joint with square opening

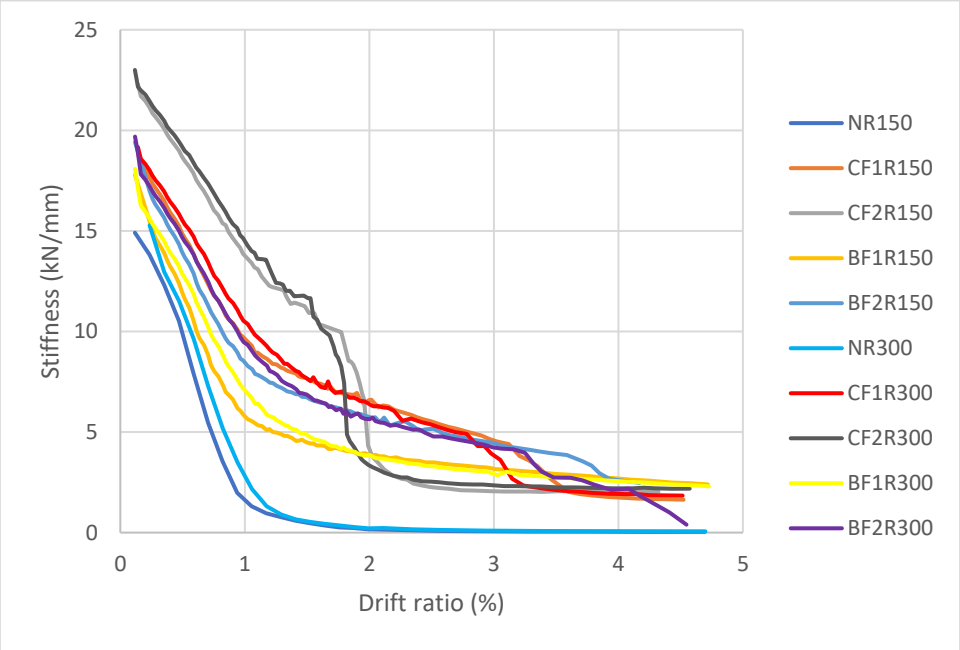

Figure 6.26 Stiffness degradation against drift ratio curve for retrofitted joint with rectangular opening

Chapter 7

Conclusion

The presence of opening has considerably reduced the strength and stiffness of beam column joint. FRP wrapping has been shown to be a superior retrofitting approach. As a result, Effect of CFRP and BFRP retrofitting in beam column joint with opening is investigated to determine its effectiveness against normal joint. Numerical model has been validated with the published test data based on experiment conducted by Sakthimurugan, et al. (2021).

For parametric study, two opening shapes square (150mm x 150mm) and rectangular (150mm x 300mm) opening in transverse beam at a distance of 150mm and 300mm from joint. The number of layers of CFRP and BFRP fabric were analyzed. From the force displacement curve obtained with varying number of CFRP and BFRP layers, it was observed that CFRP and BFRP retrofitted joint with 2 layers of CFRP fabric performed well compared to that of 1 layer of CFRP and BFRP fabric. CFRP retrofitted specimens has higher strength, stiffness and energy dissipation compared to that of BFRP retrofitted specimens, but ductility is more for BFRP retrofitted model. Hysteretic response curves showed that ultimate loads and deformation capacities for models retrofitted with CFRP are significantly higher than for BFRP retrofitted and normal beam column joint. This behavior is primarily due to the increased joint confinement caused by externally bonded CFRP fabric. All joints rehabilitated using the proposed strengthening system dissipate more energy than the normal joint when subjected to large lateral displacements thus ensuring the structure's safety. BFRP retrofitted specimens degrade at a slower rate than that of CFRP retrofitted and normal beam column joint. All the retrofitted joints have higher load carrying capacity than that of normal joint.

Each retrofitting material has its own advantages and disadvantages. While retrofitting, materials should be selected in accordance with the strengthening objective. For example, for more strength and stiffness CFRP retrofitting is to be adapted and for more ductile and low stiffness degradation BFRP retrofitting is to be used. When compared to BFRP, CFRP is significantly more expensive. Therefore, it is more cost-effective to use BFRP fabric for seismic resistance since it has more ductile nature.

References

1. ACI 318M-11 (2011), "Building Code Requirements for Structural Concrete and Commentary", Reported by ACI Committee 318, American Concrete Institute, Farmington Hills, Michigan.
2. ACI 352R-02 (2002), "Recommendations for Design of Beam-Column Connections in Monolithic Reinforced Concrete Structures", Reported by Joint ACI-ASCE Committee 352,American Concrete Institute, Farmington Hills, Michigan.
3. AbuTahnat Y. B., Dwaikat M. M. S., and Samaaneh M. A. (2018). "Effect of using CFRP wraps on the strength and ductility behaviors of exterior reinforced concrete joint." *Composite Structures*, 201, 721–739.
4. Amin, S., Elwan, S. K., Elzeiny, S., Hamad, M., & Deifalla, A. (2021). Numerical modeling the effect of an opening on the behavior of exterior beam-column connections under cyclic loading. *Journal of Building Engineering*, *40*, 102742.
5. Al-Rousan, R. Z., Alhassan, M. A., and Al-omary, R. J. (2021). "Response of interior beam-column connections integrated with various schemes of CFRP composites." *Case Studies in Construction Materials*, Elsevier Ltd., 14, 00488
6. Elsanadedy, H. M., Al-Salloum, Y. A., Alrubaidi, M. A., Almusallam, T. H., Siddiqui, N. A., and Abbas, H. (2021). "Upgrading of precast RC beam-column joints using innovative FRP/steel hybrid technique for progressive collapse prevention." *Construction and Building Materials*, Elsevier Ltd, 268(32), 121130.
7. Ilia, E., and Mostofinejad, D. (2019). "Seismic retrofit of reinforced concrete strong beam–weak column joints using EBROG method combined with CFRP anchorage system." *Engineering Structures*, Elsevier, 194(January), 300–319.
8. Lee, W. T., Chiou, Y. J., and Shih, M. H. (2010). "Reinforced concrete beam-column joint strengthened with carbon fiber reinforced polymer*." Composite Structures*, Elsevier Ltd, 92(1), 48–60.
9. Li, M., Shen, D., Yang, Q., Cao, X., Liu, C., & Kang, J. (2022), "Rehabilitation of seismic-damaged reinforced concrete beam-column joints with different corrosion rates using basalt fiber-reinforced polymer sheets", *Composite Structures*, 289, 115397.

10. Mahmoud, M. H., Afefy, H. M., Kassem, N. M., and Fawzy, T. M. (2014). "Strengthening of defected beam-column joints using CFRP." *Journal of Advanced Research*, 5(1), 67–77.
11. Mahmoud R., M. Ashkan Torab (2019), Retrofitting external RC beam-column joints of an ordinary MRF through plastic hinge relocation using FRP laminates, *Structures*, 22, , Pages 65-75.
12. Muhammad N.S. Hadi, Tung Minh Tran (2014), Retrofitting nonseismically detailed exterior beam–column joints using concrete covers together with CFRP jacket, *Construction and Building Materials*, 63, Pages 161-173.
13. Obaidat, Y. T., Abu-Farsakh, G. A. F. R., and Ashteyat, A. M. (2019). "Retrofitting of partially damaged reinforced concrete beam-column joints using various plate-configurations of CFRP under cyclic loading." *Construction and Building Materials*, Elsevier Ltd, 198, 313–322.
14. Pohoryles, D. A., Melo, J., Rossetto, T., D'Ayala, D., and Varum, H. (2018). "Experimental Comparison of Novel CFRP Retrofit Schemes for Realistic Full-Scale RC Beam–Column Joints." *Journal of Composites for Construction*, 22(5), 04018027.
15. Rodríguez, V., Guerrero, H., Alcocer, S. M., and Tapia-Hernández, E. (2021). "Rehabilitation of heavily damaged beam-column connections with CFRP wrapping and SFRM casing." *Soil Dynamics and Earthquake Engineering*, 145(March).
16. Singh, V., Bansal, P. P., Kumar, M., and Kaushik, S. K. (2014). "Experimental studies on strength and ductility of CFRP jacketed reinforced concrete beam-column joints." *Construction and Building Materials*, Elsevier Ltd, 55, 194–201.
17. Saleh, A., Hamad, M., Elzeny, S., Elwan, S. K., & Deifalla, A. (2017). The Behavior of RC Exterior Beam-Column Joint with Nearby Beam Unreinforced Web Opening under Cyclic Loading–Experimental Study. *IOSR Journal of Mechanical and Civil Engineering (IOSR-JMCE)*, *14*(4), 22-30.
18. Sabra, M. Y., Temsah, Y. A., Baalbaki, O. M., & Saleh, A. Z. (2018). Repair of Damaged Prestressed Concrete Beams Using CFRP Fabric and Stitching Techniques. *International Journal of Civil Engineering and Technology*, *9*(10), 427-440.
19. Sakthimurugan, K., & Baskar, K. (2021). Experimental investigation on rcc external beam-column joints retrofitted with basalt textile fabric under static

loading. *Composite Structures*, *268*, 114001.

20. Uma, S. R., and Prasad. (2015). “Seismic Behavior of Beam Column Joints in Reinforced Concrete Moment Resisting Frames.” *Earthquake*, 2(7), 1–36.
21. Wang, G. L., Dai, J. G., and Bai, Y. L. (2019). “Seismic retrofit of exterior RC beam-column joints with bonded CFRP reinforcement: An experimental study.” *Composite Structures*, Elsevier Ltd, 224, 111018.